scientific reports

Check for updates

OPEN

Designing a multi-epitope vaccine against African swine fever virus using immunoinformatics approach

Dhithya Venkateswaran[1], Anwesha Prakash[1], Quynh Anh Nguyen[1], Roypim Suntisukwattana[1], Waranya Atthaapa[1], Angkana Tantituvanont[2] & Dachrit Nilubol[1]✉

African swine fever (ASF) is a highly contagious and fatal haemorrhagic disease affecting domestic and wild pigs, with no effective vaccine currently available. The lack of an effective vaccine has hindered global ASF control efforts, leading to devastating economic losses in the swine industry. Traditional vaccine development approaches have faced challenges due to ASFV's genetic complexity and immune evasion strategies. Therefore, this study aims to leverage immunoinformatic approaches to facilitate acceleration of the early stages of vaccine development, optimizing resource utilization and time efficiency while providing a rational design for a potent multi-epitope vaccine against ASFV. In this study, a multi-epitope vaccine against ASFV was designed using an in-silico approach incorporating epitopes from conserved ASFV genes - B646L (p72), CP204L (p30), E183L (p54) and EP402R (CD2v). Promising epitopes that were antigenic and non-allergenic were used for the vaccine construct along with suitable adjuvant and linkers. Further analyses of the construct interpreted the physico-chemical properties, secondary and tertiary structure prediction and validation. The docking and molecular dynamics analysis of the docked complex (vaccine construct and SLA-1 0401) were performed. The docking analysis demonstrated that the vaccine construct binds well with SLA-1 0401 and the molecular dynamics analysis confirmed its strong binding affinity. The vaccine construct was confirmed as stable through normal mode analysis (NMA). Immune simulations demonstrated that this multi-epitope vaccine construct generates a strong adaptive immune response including both humoral and cell-mediated immunity. The sequence of the vaccine construct was further codon optimized with better CAI and GC content, for enhanced expression in the host *Sus scrofa*. Finally, the optimized sequence of vaccine construct was cloned into the plasmid pVAX1-eGFP. These in-silico results prove that the designed multi-epitope vaccine is potentially effective and warrants for further in vitro and in vivo studies to confirm the efficiency of the vaccine against ASFV.

Keywords African swine fever virus, Multi-epitope, Vaccine, In-silico approach, Efficacy

African swine fever (ASF) is a highly contagious haemorrhagic and deadly viral disease of domestic and wild pigs. The disease, caused by ASF virus (ASFV), is characterized by high fever, cyanosis of peripheral organs, anorexia, fatigue, lethargy and ataxia whose mortality rate can approach 100%[1]. ASFV variants can be classified as highly virulent, moderately virulent, or low virulent based on the severity of clinical symptoms and the mortality rate. The mortality rates are 100%, 30–70% and < 30% in the highly virulent, moderately virulent and less virulent ASFV isolates, respectively[2].

ASFV, the only member of the *Asfaviridae* family, is a large nucleocytoplasmic double-stranded enveloped icosahedral DNA virus[3]. ASFV possesses a large genome that varies from 170 kbp to 193 kbp, which comprises of 180 to 200 genes. To date, 60 structural and 100 non-structural proteins that are actively involved in one or more stages of the ASFV infection cycle have been recorded[4,5]. Though many of the ASFV proteins are unessential for viral replication, they have key roles in interactions with the host to facilitate its survival and transmission. The ASFV is made of 5 layers comprising of Outer envelope, inner envelope, capsid, core shell and nucleoid with different genes and their encoded proteins spanning each layer. The stages of ASF infection begins with adsorption and internalization (macropinocytosis or clathrin mediated endocytosis), followed by endosomal

[1]Swine Viral Evolution and Vaccine Development Research Unit, Department of Veterinary Microbiology, Faculty of Veterinary Science, Chulalongkorn University, Bangkok 10330, Thailand. [2]Department of Pharmaceutic and Industrial Pharmacies, Faculty of Pharmaceutical Sciences, Chulalongkorn University, Bangkok 10330, Thailand. ✉email: dachrit@gmail.com

trafficking, viral uncoating, viral biosynthesis (transcription, translation, replication), virion assembly and egress[6]. Different genes and the encoded proteins are involved in different phases of infection on the basis of which the genes are expressed as early (4–8 hpi), intermediate (8–16 hpi) or late genes (16–24 hpi)[5].

ASFV was classified into 24 genotypes based on partial B646L gene (encoding the P72 protein). The traditional classification of African swine fever virus (ASFV) based on the p72 gene and identification of 24 different genotypes was prone to inaccuracies due to its reliance on a limited set of amino acid changes, which could be impacted by sequencing errors. A recent publication suggested that ASFV should be classified into only 7 genotypes, considering the entire proteome of the virus, offering a more comprehensive view of its genetic diversity[7]. Presently, all 24 ASFV genotypes are found in sub-Saharan Africa, but only genotypes I and II have been reported outside the Africa continent, mainly in Europe and Asia[8]. First identified in Kenya in 1921, ASF spread across sub-Saharan Africa and became endemic[9]. Genotype I reached Europe in 1957, re-entered in 1960 through Portugal, and later spread to South America and the Caribbean, though it was eradicated from most regions, except Sardinia[10,11]. Genotype II emerged in Georgia in 2007, triggering major outbreaks across Europe and Asia of which China reported its first case in 2018. By 2024, ASF, especially genotype II, has spread to over 50 countries, posing a threat to swine industry worldwide[12].

Due to the lack of an effective and safety vaccine, prevention and control measures therefore rely on the early detection and depopulation of infected or affected animals[13]. The development of effective vaccines against ASFV has been a major focus of research. Several traditional and new generation vaccines have been extensively experimented against ASFV. However, the deployment in field situations remains a challenge. Inactivated vaccines have been proved to be completely ineffective against ASFV, even after pairing with adjuvants[14,15]. The inactivated vaccines failed to induce both humoral and cell mediated immunity, consequently providing no protection against experimental challenge. Due to the complex genome structure of ASFV does make it more favourable to the development of live attenuated virus vaccines (LAVs)[16], but this advantage is tempered by safety concerns. LAVs are one of the vaccine strategies being explored to combat ASFV, and they can indeed be classified into different categories based on the methods used to attenuate the virus, including naturally attenuated (NA-LAV), attenuated through cell passages (AC-LAV), and gene deletion (GD-LAV) vaccines. Naturally attenuated strain, for instance, OURT88/3, had demonstrated up to 85% protection with booster immunization[17]. Despite conferring high protective efficacy, pigs vaccinated with the naturally attenuated LAVs, OURT88/3, displayed chronic symptoms and persistent infection. AC-LAV became completely attenuated, but failed to protect pigs against ASFV challenge, following 110 successive passages in Vero cells[18,19]. GD-LAV have become one of the more favourable approaches for developing vaccines against ASFV, particularly when compared to other methods, NA-LAV and AC-LAV. GD-LAVs have shown considerable promise due to their genetic stability, predictability, and improved safety profile[20]. Albeit GD-LAVs have many advantages, they also come with disadvantages and safety concerns that must be carefully addressed. The main risks associated with GD-LAVs for ASFV include reversion to virulence, virus carriers and transmission risks, side effects, and inconsistent efficacy. These factors, along with the need to balance safety and efficacy, continue to limit the widespread clinical application of ASFV LAVs[4,17].

Due to safety concerns associated with live attenuated vaccines, a more novel approach involving subunit, DNA, and viral vector vaccines, with enhanced safety profiles are considered[21]. Subunit vaccines developed using p30, p54, p72, p22, CD2v and pp62 individually and as combinations were able to induce neutralizing antibodies (NAbs), however, these NAbs were not sufficient to confer protection, failing to induce cell mediated immunity[21–24]. Other ASFV envelope and intramembrane proteins, such as p12, and D117L, also induced NAbs, helping block viral invasion and release but complete protection was not observed[25]. Incomplete immune protection, limited durability of immunity further hinders the application of subunit vaccines. DNA vaccines are known to induce robust T - cell responses in hosts.

However, their efficacy in protecting against ASFV remains limited[17,26], and it can be improved by targeting antigens to specific cells[27]. Various recombinant viruses have been used to develop viral vector-based vaccines against ASFV. p72, p30, p54, E183L, E199L, EP153R, F317L, and MGF505-5R recombinant viruses, were constructed using poxvirus and adenovirus vectors. Similarly, an alphavirus vector platform was used to deliver replicon particles (RPs) expressing ASFV antigens in swine[28]. Additionally, a Semliki Forest virus (SFV) vector expressing ASFV antigens p32 (SFV-p32) and p54 (SFV-p54) was developed to assess its potential as a vaccine candidate[29]. However, despite the promising immunogenicity data, viral vector vaccination have shown limited protection after challenge with virulent ASFV, and in some cases resulted in enhanced disease[30], together with adverse effects including anaphylaxis, allergic reactions etc[21].

Multi-epitope vaccines could be a promising prophylactic and therapeutic tool. Firstly, the epitopes (Helper T-cell, Cytotoxic T-cell and B-cell) of characterised viral proteins exposed to the virus surface are selected for inducing both humoral and cell-mediated response, successfully targeting multiple potential antigens simultaneously. Secondly, MHC restricted epitopes that present the antigen to the TCRs of the T-cells can also be used[31]. Thirdly, this multi-epitope vaccine construct has minimal side effects and lesser antigenic load whilst targeting a wide range of antigens. Selective addition and removal of antigenic epitopes is a significant strength of this vaccine[32,33].

Few multi-epitope vaccines have also been designed against ASFV using different genes of interest with varying immune responses on the basis of the various analysis performed[31,33].

ASFV encodes approximately 180 to 200 genes, many of which play crucial roles in viral infection, immune evasion, and virulence, making them potential vaccine targets. However, not all genes are equally suitable for vaccine development[34]. The selection of target genes in this study was guided by key criteria, including high conservation across ASFV strains to ensure broad vaccine efficacy, essential roles in viral survival, replication, and virulence, strong immunogenicity to elicit protective immune responses, and known involvement in host immune modulation[35]. Since incorporating a large number of genes could introduce complexities in vaccine

stability, expression efficiency, and immune processing, we aimed to use a limited set of genes while ensuring that the selected genes provided a diverse and comprehensive set of immunogenic epitopes capable of inducing both humoral and cell-mediated immunity. Based on these criteria, four highly conserved ASFV genes—B646L (p72)[36], CP204L (p30)[37], E183L (p54)[38], and EP402R (CD2v)[39]—were selected for vaccine design. These genes have been widely utilized in the development of ASFV vaccine constructs, demonstrating their significance in eliciting an immune response and contributing to vaccine efficacy[23,40,41]. B646L encodes p72, the major capsid protein that is indispensable for viral entry, internalization, and virion assembly[11]. As the most abundant structural protein of ASFV, p72 plays a key role in virion stability and host cell invasion[11]. Due to its surface exposure, it is a key target for host immune recognition, eliciting neutralizing antibody responses that can help limit viral spread. E183L encodes p54, which facilitates intracellular transport and viral egress by binding to the LC8 chain of dynein, enabling movement of the virus within the host cell[5]. Additionally, p54 is essential for membrane precursor and core shell assembly, making it a crucial component in the viral replication cycle[42]. Its presence during early infection stages allows it to act as a potent antigen, stimulating an immune response that can interfere with viral propagation[43]. CP204L encodes p30, a virulence-associated protein that is critical for viral entry and internalization, while also stimulating the production of virus-neutralizing antibodies. P30 has been shown to play a role in immune evasion by interfering with host signalling pathways, and its immunogenic nature makes it an attractive candidate for vaccine development[44]. EP402R encodes CD2v, a protein involved in immune modulation, mediating hemadsorption and immune cell interactions[45]. CD2v disrupts the host immune response by impairing lymphocyte adhesion and immune synapse formation, allowing ASFV to evade immune detection[46]. However, its immunogenic properties make it a strong candidate for inducing a protective cell-mediated immune response when used as a vaccine antigen[47]. The inclusion of these genes in the vaccine design aims to stimulate a comprehensive immune response in the host, incorporating both humoral and cell-mediated immunity. The selection of structural and virulence-associated proteins ensures that the vaccine elicits neutralizing antibodies to block viral entry while also activating cytotoxic T lymphocytes (CTLs) to target infected cells. By presenting highly antigenic and conserved viral epitopes, this vaccine construct is expected to induce a robust and long-lasting immune response, providing broad protection against ASFV infection. The selection of epitopes of genes p72, CD2v, and p30 in this study is supported by previous work[48], which employed a similar combination of ASFV proteins (p72, CD2v, p30, and pB602L) for epitope prediction and subsequent immunization in mice. Their study demonstrated that the constructed nanoparticle-based vaccine can elicit a robust T-cell response, with high antibody levels against ASFV persisting for over 231 days. While their approach involved experimental validation through wet-lab studies, our study focuses entirely on an in-silico framework for computational design and immunogenic epitope evaluation. Additionally, the inclusion of p54 in our construct enhances its antigenic potential, further strengthening its suitability as a vaccine candidate.

However, with such a large number of proteins and a proportionally large number of epitopes that could exist for each protein, ASFV epitope mapping is a cumbersome task. A trial-and-error procedure time consuming and expensive[49]. To overcome this, immunoinformatics, an insilico approach driven by computational methodologies can be used. Application of immunoinformatic tools for epitope prediction, analysis, and mapping, as well as for predicting antigen-antibody interactions and designing vaccines, can streamline the vaccine development process and significantly reduce the reliance on traditional trial-and-error methods which are time and resource intensive. This makes immunoinformatics a game changer in vaccine development[50,51].

In that context, this research aims to design a multi-epitope vaccine against ASFV using immunoinformatics approach and evaluate the effectiveness of the vaccine candidate in inducing a protective immune response against ASFV in swine populations.

Materials and methods

In this study, we employed an in-silico approach for the design and evaluation of potential multi-epitope vaccine, utilizing computational tools and bioinformatics resources to predict and analyze antigenic peptides essential for effective vaccine development. Our methodology integrates various software and web servers essential for different stages of the vaccine design process. To facilitate replication and further exploration, we have included a table with detailed links to all the software and web servers used in this immunoinformatics study, ensuring consistency and reproducibility in vaccine design endeavours (Table 1).

Retrieval of ASFV sequences

The ASFV protein sequences used in the study were retrieved from the NCBI – GenBank database. The protein sequences were retrieved from the complete genomes of representative isolates from China, Korea, Vietnam, the Philippines, Thailand, and the Georgia 2007/1 reference strain. In total, 29 publicly available whole genome sequences were selected from the NCBI–GenBank database guided by the methodology described by Salman et al. (2024)[52]. The selected ASFV proteins included B646L (p72), CP204L (p30), E183L (p54), and EP402R (CD2v) — all of which are known to play key roles in viral replication and immune response activation.

Linear B lymphocyte epitope prediction

The protein sequences of ASFV were used to screen for linear B lymphocyte (BL) epitopes. The tool BepiPred Linear Epitope 2.0 (BLE) in Immune Epitope Database (IEDB) analysis resource (http://tools.iedb.org/bcell/) was used to generate linear BL epitopes.

Linear helper T lymphocyte epitope prediction

The protein sequences of ASFV were used to screen for helper T cell epitopes by assessment of the predicted MHC II binding using IEDB analysis resource: MHC II Binding Prediction (http://tools.iedb.org/mhcii/) set with NetMHCIIpan 4.1 EL (recommended epitope predictor – 2023.09).

Stage	Software/webserver	Link
Sequence retrieval	NCBI - GenBank	https://www.ncbi.nlm.nih.gov/genbank/
Sequence alignment	Clustal omega	https://www.ebi.ac.uk/jdispatcher/msa/clustalo
B cell epitope prediction	IEDB - BepiPred linear epitope 2.0	http://tools.iedb.org/bcell/
CD4 + epitope prediction	IEDB - MHC II binding prediction	http://tools.iedb.org/mhcii/
CD8 + epitope prediction	IEDB - Proteasomal cleavage/ TAP transport/ MHC class I combined predictor tool	http://tools.iedb.org/processing/
Antigenicity prediction	VaxiJen v.2.0	https://www.ddg-pharmfac.net/vaxijen/VaxiJen/VaxiJen.html
Allergenicity prediction	AllergenFP v.1.0	https://ddg-pharmfac.net/AllergenFP/
Conservancy prediction	IEDB conservancy analysis	http://tools.iedb.org/conservancy/
Cross-reactivity	BLASTp	https://blast.ncbi.nlm.nih.gov/
Physicochemical analysis	ExPasy ProtParam	https://web.expasy.org/protparam/
Secondary structure prediction	PSIPRED V3.3	http://bioinf.cs.ucl.ac.uk/psipred/
	GOR4	https://npsa-pbil.ibcp.fr/NPSA/npsa_gor4.html
Tertiary structure modelling	AlphaFold3	https://alphafoldserver.com/
Tertiary structure refinement	Galaxy Refine server	https://galaxy.seoklab.org/cgi-bin/submit.cgi?type=REFINE
Structural validation	ERRAT	https://saves.mbi.ucla.edu/
Structure visualization	PyMOL	https://www.pymol.org/
Molecular docking	ClusPro server	https://cluspro.org/home.php
Receptor cleaning	ChimeraX	https://www.rbvi.ucsf.edu/chimerax/
Molecular dynamics	Desmond simulation package from Schrödinger LLC	https://www.schrodinger.com/platform/products/desmond/
	PRODIGY	https://rascar.science.uu.nl/prodigy/
Normal mode analysis	iMODS	https://imods.iqf.csic.es/
Immune response profile	C-ImmSim server	https://kraken.iac.rm.cnr.it/C-IMMSIM/index.php
Codon optimization	Vector builder	https://en.vectorbuilder.com/tool/codon-optimization.html
Insilico cloning	Novobuilder tool	https://www.novoprolabs.com/plus/novobuilder/

Table 1. Software and webservers used in the study and their respective weblinks.

Linear cytotoxic T lymphocyte epitope prediction

The protein sequences of ASFV were used to screen for Cytotoxic T lymphocytes using IEDB analysis resource: proteasomal cleavage/ TAP transport/ MHC class I combined predictor tool in IEDB (IEDB recommended prediction method) (http://tools.iedb.org/processing/). In addition to antigen processing (proteasomal cleavage), TAP (transporter associated with antigen processing protein) transport, MHC class I binding, and T cell receptor-MHC interaction are included in the prediction outcomes for potential CTL epitopes. Since no potential CD8 + epitope could be shortlisted based on allergenicity and antigenicity, this category was excluded.

Antigenicity, allergenicity and conservancy prediction of shortlisted epitopes

Predicted BL, HTL, and CTL epitopes were evaluated for antigenicity using the VaxiJen v.2.0 server (https://www.ddg-pharmfac.net/vaxijen/VaxiJen/VaxiJen.html). The retrieved B-cell, CD4 + and CD8 + epitopes were submitted in FASTA format as single file. Based on previous methodology and research articles by Doytchinova et al. (2007) and Tahir ul Qamar et al. (2019) respectively, which utilized the VaxiJen v2.0 server for viral antigenicity prediction, the target organism for our multi-epitope vaccine construct was set as "virus," with a threshold value of 0.5[53,54]. The antigenic epitopes were tested for allergenicity using the insilico tool AllergenFP v.1.0 (https://ddg-pharmfac.net/AllergenFP/). The same antigenicity and allergenicity analyses were followed for the vaccine construct as well. The epitopes that qualified as probable antigen and probable non-allergen were submitted to the IEDB Conservancy Analysis tool to assess their conservation across the corresponding amino acid sequences of p72, p54, p30, and CD2v proteins extracted from the 29 ASFV genomes, using the reference protein sequences retrieved from the NCBI database as a baseline[55].

Construction of multi-epitope vaccine construct

The ASF vaccine was constructed using the evaluated epitopes of the proteins p30, p54, CD2v and p72. The epitopes were lined up in the order of HTL epitopes followed by BL epitopes. GPGPG linker was used to link each epitope with the subsequent one[56,57]. CpG-ODN 2007, a Class B CpG oligonucleotide, serves as the adjuvant in this study. These unmethylated CpG motifs mimic microbial DNA, effectively stimulating the immune system. CpG-ODN 2007 is a preferred ligand for porcine and bovine Toll-like receptor 9 (TLR9), as it elicits a potent immune response while exhibiting lower toxicity compared to other adjuvants[58]. CpG-ODN 2007 was added at the beginning and end of the vaccine construct as the adjuvant to increase the immunogenicity of the vaccine[59,60]. The adjuvant at the beginning and end was connected with the first and the last epitope of the lineup respectively using EAAAK linker[61]. The construct was submitted for allergenicity and antigenicity prediction in AllergenFP and Vaxigen server respectively. The vaccine construct was also checked for cross reactivity by analyzing the sequence similarity to swine proteins (*Sus scrofa*, *Sus scrofa domestica*, *Sus scrofa domesticus*) with NCBI-BLASTp (https://blast.ncbi.nlm.nih.gov/). Default parameters were used[56].

Physiochemical analysis of vaccine construct

The physiochemical parameters of the vaccine construct were analyzed using ExPasy ProtParam (https://web.expasy.org/protparam/). The physicochemical properties include molecular weight, theoretical pI, extinction coefficient, aliphatic index, instability index, total number of negative and positively charged amino acids, estimated half-life and grand average of hydropathicity (GRAVY) score[62]. Additionally, SOLpro server was also used to predict the solubility of the vaccine construct[63].

Secondary structure prediction and validation of the construct

The secondary structure of the multi-epitope vaccine construct was predicted by PSIPRED V3.3 (http://bioinf.cs.ucl.ac.uk/psipred/) that uses two feed-forward neural networks and GOR4 (https://npsa-pbil.ibcp.fr/cgi-bin/npsa_automat.pl?page=/NPSA/npsa_gor4.html) for percentage of the secondary structure composition of the structure[49,51].

Tertiary structure prediction and validation of the construct

The tertiary structure was initially modelled with the using **AlphaFold3**, a deep-learning-based protein structure prediction tool (https://alphafoldserver.com/)and further refined using the Galaxy Refine server (https://galaxy.seoklab.org/cgi-bin/submit.cgi?type=REFINE). To ensure structural validity, the refined structures were assessed using ERRAT (https://saves.mbi.ucla.edu/). The 3D protein structure of the vaccine construct was further evaluated using Ramachandran Plot generated through PROCHECK (https://saves.mbi.ucla.edu/). Visualization of the final structure was performed with ChimeraX[31].

Molecular docking

The refined structure of the vaccine construct was docked with the cleaned structure of the swine major histocompatibility complex SLA-1 0401 (PDB ID: 3QQ3), retrieved from the RCSB-PDB server, using the ClusPro server (https://cluspro.org/home.php). The 3QQ3 PDB file, which represents the crystal structure of the swine MHC class I SLA-1 0401 complexed with peptides of swine-origin influenza A H1N1 virus, was cleaned using ChimeraX. During this process, the β-2-microglobulin and peptide OF SLA-10,401-S-OIVNW9 were removed, leaving only the heavy chain of SLA-10,401, which is the primary component responsible for binding and presenting antigens[31]. The selected ASFV multi-epitope and SLA-1 0401 complex and the amino acid interactions was viewed in PyMOL.

Molecular dynamics simulation and normal mode analysis

The ASFV multi-epitope vaccine docked with SLA-1 0401 was submitted to PRODIGY server for evaluation of the binding strength and stability (https://rascar.science.uu.nl/prodigy/).

Molecular dynamics (MD) simulations were performed using the Desmond simulation package from Schrödinger LLC[64]. The simulations were conducted under the NPT ensemble, maintaining a temperature of 300 K and pressure of 1 bar throughout all runs. Each simulation lasted 100 ns with a relaxation time of 1 ps for both the receptor and receptor complex. The OPLS_2005 force field was applied to all systems. Long-range electrostatic interactions were calculated using the Particle Mesh Ewald (PME) method, with a Coulomb cutoff of 9.0 Å. Water molecules were explicitly modelled using the Simple Point Charge (SPC) model. Trajectories were saved at 4.8 ps intervals for subsequent analysis. The behaviour and interactions of the protein were examined using the Simulation Interaction Diagram tool, which is part of the Desmond package. To assess the stability of the simulations, the Root Mean Square Deviation (RMSD) of the protein's atomic positions was monitored over time[65].

Through Normal mode analysis (NMA), the stability, flexibility and atomic/molecular movement of the docked complex was studied using iMODS webserver (https://imods.iqf.csic.es/)[66].

Immune response profile of multi-epitope ASF vaccine

The immune response generated by the constructed multi-epitope ASF vaccine was simulated by the C-ImmSim server (kraken.iac.rm.cnr.it/C-IMMSIM/index.php). The server uses position-specific scoring matrix (PSSM) to evaluate immunological interactions through an agent-based model and machine learning. The default parameters were used for the study[63].

Codon optimization

Vector builder (https://en.vectorbuilder.com/tool/codon-optimization.html) was used for codon optimization of the vaccine construct. Codon optimization is performed to enhance the expression of any given sequence in a specific host organism. The selected host organism was Sus Scrofa (pig).

Insilico cloning

Novobuilder tool (https://www.novoprolabs.com/plus/novobuilder/) of NovoPro Bioscience Inc. was employed to insert and clone the adapted vaccine sequence into pVAX1-eGFP vector between EcoRI and XbaI restriction sites.

Results

Retrieval of ASFV sequences

The target protein sequences were retrieved from the NCBI database. The sequences of B646L (p72), CP204L (p30), E183L (p54), and EP402R (CD2v) from the 29 ASFV isolates were aligned using Clustal Omega. The multiple sequence alignment revealed a high degree of sequence identity across all strains, confirming the

conserved nature of these proteins. Based on this observation, the aligned sequences were used for downstream epitope prediction analyses, including B-cell, helper T-cell (HTL), and cytotoxic T-cell (CTL) epitope screening.

Linear B lymphocyte epitopes prediction

B lymphocytes drive humoral immunity by production of antibodies. however it also plays an important role in amplification of cell-mediated immune response along with T lymphocyte[67]. In both in vivo and in vitro studies, antibodies have demonstrated potential protective effects through various mechanisms, such as complement-mediated cell lysis and antibody-dependent cellular cytotoxicity[68]. These findings highlight the potential of antibodies to offer protection against ASF. Consequently, BL epitopes were incorporated into the vaccine design. BepiPred Linear Epitope 2.0 (BLE) tool found in Immune Epitope Database (IEDB), was used to generate linear B-Cell epitopes. BepiPred-2.0 server uses random forest algorithm to predict B-cell epitopes. The threshold value was set at 0.5. The epitope was predicted using residues with scores above the threshold (default value is 0.5). The table thus generated included the B-cell epitopes and their positions in the protein (Table 2).

Linear helper T lymphocyte epitope prediction

Helper T lymphocytes, or CD4 + T cells, play a critical role in the immune system by activating other immune cells such as B cells, which produce antibodies; cytotoxic T cells (CD8 + T cells), which kill infected cells; and macrophages, which engulf and destroy pathogens. Additionally, they secrete cytokines, signalling molecules that shape and coordinate the immune response, ensuring a robust and targeted defence against infections and other threats. This is achieved by interacting with MHC class II molecules (SLA II in swine) on antigen presenting cells (APC). Of the two classes MHC (SLA in swine): MHC I interact with endogenous peptides and MHC II interacts with exogenous peptides[69]. For MHC-II epitope prediction, HLA molecules were used due to the absence of SLA-II alleles in the IEDB-recommended MHC-II binding prediction tools[33,70]. Owing to the physiological similarity between humans and pigs, common human MHC II alleles (HLA-DRB1*01:01, HLA-DRB1*03:01, HLA-DRB1*04:01) that are orthologs to their swine counterpart alleles were used to predict epitope peptides[31,51,71]. The epitopes and their binding affinity with MHC II alleles were determined through IEDB recommended MHC II Binding Prediction set - NetMHCIIpan 4.1 EL (recommended epitope predictor – 2023.09) in the IEDB server. Helper T-lymphocyte (HTL) epitopes with percentile rank < 10.0 and high score (denotes good binding), and length of 15 amino acids were considered for further antigenicity and allergenicity prediction[72]. All the shortlisted epitopes are 15-mers in length with score ranging between 0.45 and 0.91 and rank ranging between 0.2 and 2.9 which are all less than 10 (Table 3).

Linear cytotoxic T lymphocyte epitope prediction

Cytotoxic T lymphocytes are important effector cells of the adaptive immune system, which are known to interact with MHC class I molecules present on antigen presenting cells. In swine immunity, MHC-I interacting with CTLs are referred to as SLA Class I. These CTLs cause cytotoxicity to virus-infected cells through the action of perforins, granzymes and cytotoxic granules. Antigens undergo proteasomal cleavage to become peptides and are transported by TAP (transporter associated with antigen processing protein) from cytosol to the endoplasmic reticulum (ER) and finally presented on MHC class I molecules. In addition to antigen processing (proteasomal cleavage), TAP transport, MHC class I binding, then T cell receptor-MHC interaction is included in the prediction outcomes for potential CTL epitopes. Since the aim is to produce a vaccine for swine, common SLA class I molecules (SLA-1, -2, and − 3) are utilized in the prediction. The predicted epitopes were filtered using these parameters: epitope length 11 residues, IC50 < 500 nM (ideal binders, a threshold associated with immunogenicity), TAP score > 1.0, proteasome-processing score > 1.0, and those covering the MHC I SLA alleles. Proteasome-processing scores evaluate the generation of peptides with corresponding C-terminus. TAP transport score calculates the generation of peptide or N-terminally extended precursors. Both the proteasome-processing and TAP transport scores are predictors that were tested using TOC curves, which utilizes type positive and false positive predictions for every threshold and an area under the ROC curve is measured for the predictor's performance. Perfect predictor would score > 1. Scrutinizing based on these criteria, no epitopes were available for proteins p54 and CD2v.

Gene	B-cell epitope	Start	Stop	Length	Non-allergen TSI score	Antigen prediction score
CP204L (p30)	VIFKTDLRSSSQ	13	24	12	0.68	0.5837
E183L (p54)	GPAAAPAAASAPAHPAEPYTTVT-TQNTASQTMSAIENLRQRNTYTHKDL	132	180	49	0.8	0.5169
EP402R (CD2v)	GKAGNFCECSNYSTS	58	72	15	0.62	0.7964
	NNSNINN	161	167	7	0.82	0.5583
B646L (p72)	MQPTHHAEISFQDRDTALPDACSSISDISPV	498	528	31	0.74	1.3437
	SNIKNVNKSYGKPDPEPTLSQI	31	52	22	0.66	1.016
	RFIAGRPSRRNIRF	380	393	14	0.6	0.8088

Table 2. The shortlisted non-allergenic and antigenic B-cell epitopes of each gene/protein and their position, length and TSI score (for allergenicity) and prediction score (for antigenicity).

Gene	Allele	Start	Stop	Core peptide	MHC II peptide for HTL	Score	Rank	Non-allergen TSI score	Antigen prediction score
CP204L (p30)	HLA-DRB1*03:01	12	26	FKTDLRSSS	EVIFKTDLRSSSQVV	0.5745	2.2	0.62	0.5142
	HLA-DRB1*03:01	11	25	FKTDLRSSS	MEVIFKTDLRSSSQV	0.5559	2.3	0.63	0.6286
	HLA-DRB1*03:01	10	24	FKTDLRSSS	KMEVIFKTDLRSSSQ	0.4612	2.9	0.66	0.6828
E183L (p54)	HLA-DRB1*04:01	146	160	YTTVTTQNT	PAEPYTTVTTQNTAS	0.905	0.2	0.63	0.5075
	HLA-DRB1*01:01	75	89	WVEVTPQPG	DQQWVEVTPQPGTSK	0.8395	0.7	0.64	0.7015
	HLA-DRB1*04:01	148	162	YTTVTTQNT	EPYTTVTTQNTASQT	0.8001	0.74	0.66	0.5561
	HLA-DRB1*04:01	160	174	MSAIENLRQ	SQTMSAIENLRQRNT	0.7665	0.96	0.66	0.8885
EP402R (CD2V)	HLA-DRB1*04:01	29	43	ITNDNNDIN	DSNITNDNNDINGVS	0.5774	2.1	0.68	0.6327
	HLA-DRB1*04:01	282	296	IYYMRPSTQ	NTPIYYMRPSTQPLN	0.4895	3.1	0.63	0.5480
B646L (P72)	HLA-DRB1*03:01	162	176	IVPGTKNAY	GRPIVPGTKNAYRNL	0.7363	1.2	0.56	0.6999
	HLA-DRB1*03:01	160	174	IVPGTKNAY	PFGRPIVPGTKNAYR	0.6578	1.6	0.51	0.5415
	HLA-DRB1*04:01	611	625	YVGSITTAD	DTDYVGSITTADLVV	0.6193	1.9	0.64	0.6277

Table 3. Table 1: the shortlisted non-allergenic and antigenic helper T-cell epitopes of each gene/protein and their position, core peptide, target allele, score, rank and TSI score (for allergenicity) and prediction score (for antigenicity).

Antigenicity and allergenicity prediction of the shortlisted epitopes

The antigenicity prediction tool - VaxiJen server was developed using Perl for its core functionality and features an HTML user interface. It employs three distinct models specifically designed to identify bacterial, viral, and tumour antigens. The antigen probability is presented as a prediction score supported by a statement indicating the submitted epitope as either "Probable Antigen" or "Probable Non-Antigen"[53]. Epitopes classified as "Probable Antigens" with a prediction score greater than 0.5 were prioritized for vaccine design to ensure a high degree of antigenicity. A higher prediction score indicates a stronger antigenic potential, which is critical for inducing a robust immune response.

The allergenicity of the epitopes was checked to ensure that no allergens are included, thereby ensuring the safety of the proposed vaccine construct. The allergenicity of proteins was calculated using the Tanimoto Similarity Index (TSI) by the in silico tool AllergenFP. TSI indicates a similarity score with allergen or non-allergen between 0 and 1 scale. TSI predicts the allergenicity of proteins by comparing their binary fingerprints alongside known allergens stored in its database. Binary fingerprints contain the properties and features of the protein sequences. By assessing the similarity between the protein and the database, the server determines the likelihood of the protein being an allergen. The calculated TSI is then compared to a predefined threshold. If the TSI exceeds the threshold, the protein is classified as a "Probable Allergen," else it is classified as a "Probable Non-Allergen.". Non-allergenic epitopes were selected from all the retrieved epitopes of ASFV.

The BL and HTL epitopes that were both antigenic and non-allergenic were selected for the construction of the vaccine (Tables 2 and 3). Since no potential CTL (CD8+) epitope could be shortlisted based on allergenicity and antigenicity prediction scores, this category was excluded from the vaccine construct (table not given). Also, all the shortlisted epitopes were found to be highly conserved in comparison to their respective amino acid sequences through the IEDB conservancy analysis server.

Construction of a multi-epitope vaccine

The vaccine construct was made of 19 epitopes comprising of 12 HTL epitopes and 7 BL epitopes connected by linkers (EAAAK linker – 2 and GPGPG linker – 17) and 2 copies of CpG-ODN-2007 adjuvants based on previous research works[59,60]. The protein sequence of the vaccine construct and the detailed quantitative description of the components of the vaccine construct has been provided in Fig. 1. The total size of the construct was 469aa residues. The vaccine construct was recorded to be "probable non-allergen" with a TSI score of 0.83 using the AllergenFP server. It was also recorded as "probable antigen" with a score of 0.6421 through the VaxiJen v.2.0 server. No sequence similarity was observed in NCBI-BLASTp, confirming absence of cross-reactivity.

Physiochemical analysis of vaccine construct

The physicochemical parameters of the multi-epitope vaccine construct were retrieved using ExPASy – ProtParam and the results are given in Table 4. The number of the amino acid in the vaccine construct is 469. The number of amino acid residues present in a sequence is proportional to corresponding molecular weight. The molecular weight in 47343.02 Da. The total number of atoms present are 6499. The number of negative (Asp + Glu) and positive amino acids (Arg + Lys) present are 31 and 34 respectively. The theoretical pI is an indication of the charge carried by the protein and thus its nature, whether acidic or basic. Amino acids with low isoelectric point (<7) are negatively charged and are hence acidic in nature. In contrast, amino acids with high isoelectric point (>7) carry positive charge and are basic in nature[73]. The pI value of the vaccine construct was predicted to be 8.24, making our construct basic in nature. This means that at a pH below 8.24, the protein will carry a net positive charge, and at a pH above 8, it will carry a net negative charge. Aliphatic index (AI) is a measure of the thermostability of the proteins which is based the relative volume occupied by the aliphatic side chains consisting of alanine, valine, leucine and isoleucine. The greater the volume occupied by aliphatic side chains, the higher will be the aliphatic index[74]. The aliphatic index is 45.16 which is a relatively low thermostability

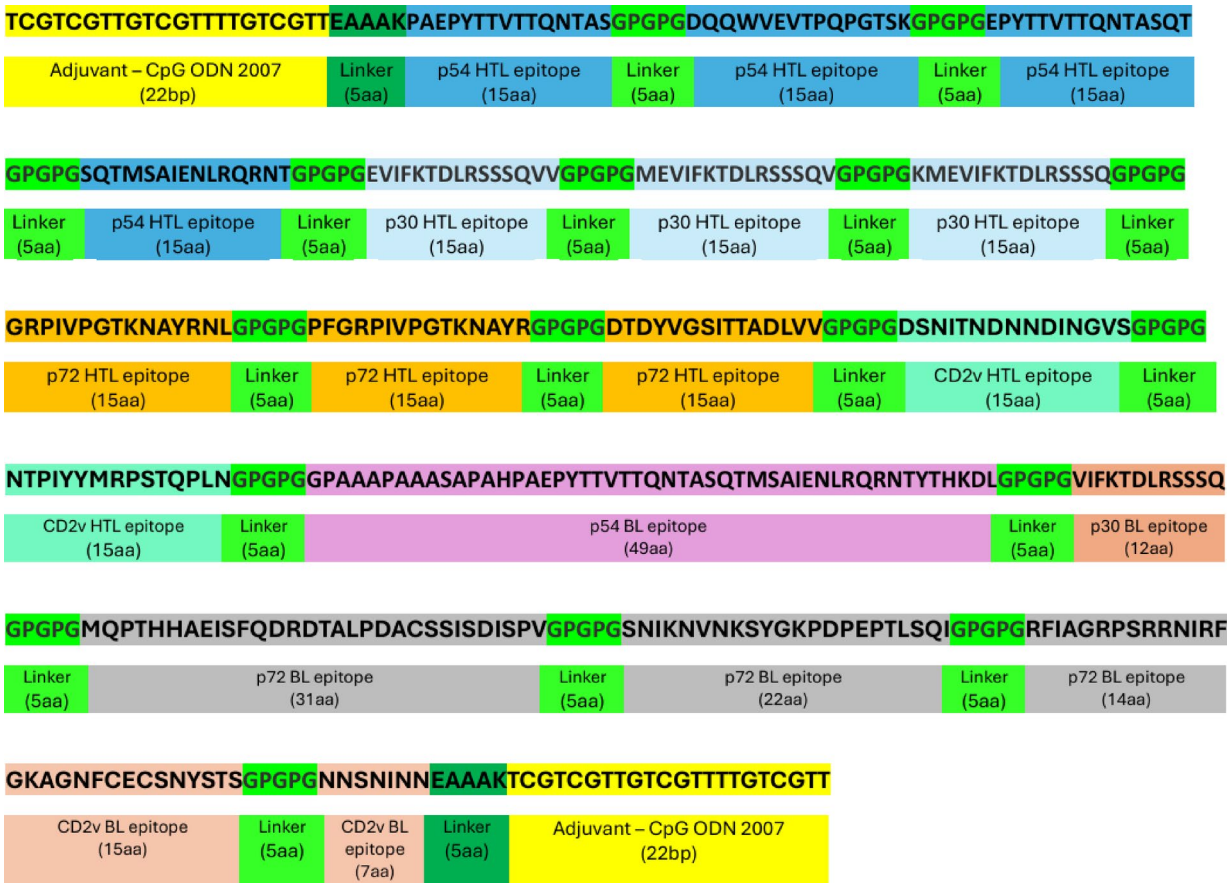

Fig. 1. Graphical representation of the multi-epitope vaccine construct, depicting the sequential arrangement of HTL and BL epitopes with linkers. The figure includes a legend for component identification and a quantitative breakdown of HTL, BL, linkers, and the adjuvant.

Number of amino acids	469
Molecular weight	47343.02
Total number of atoms	6499
Total number of negatively charged residues	31
Total number of positively charged residues	34
Theoretical pI	8.24 (> 7, basic)
Aliphatic index	45.16
Instability index	37.16 (stable)
Extinction coefficient	22,515 [Abs 0.1% (= 1 g/l) 0.476, assuming all pairs of Cys residues form cysteines] 21,890 [Abs 0.1% (= 1 g/l) 0.462, assuming all Cys residues are reduced]
Estimated half-life	7.2 h (mammalian reticulocytes, in vitro) >20 h (yeast, in vivo) >10 h (Escherichia coli, in vivo)
GRAVY	−0.655

Table 4. Physicochemical parameters of the multi-epitope construct.

value. Instability index (II) values above 40 represent unstable proteins while those with II values less than 40 denote stable proteins[75]. Our multi-epitope vaccine construct with II 37.16, is stable. Extinction coefficient is a measure of how strongly a chemical species absorbs light at a given wavelength[76]. The extinction coefficient for the construct is 22,515 and 21,890 assuming all pairs of Cys residues form cysteines or are reduced respectively. Estimated half-life of the vaccine construct is less than 10 h. GRAVY value (grand average of hydropathicity) is used to interpret the hydrophobicity value of a protein. Positive value indicates hydrophobicity and negative value indicates hydrophilicity[77]. The vaccine construct has a negative GRAVY value of -0.655 and hence is hydrophilic in nature.

$$\text{GRAVY} = \frac{\text{Hydropathy values of all the amino acids}}{\text{Sequence length}}$$

SOLpro server predicted the probability of the solubility of the vaccine construct to be 0.901279. The range of values lies between o to 1, confirming that our construct is highly soluble in water[63].

Secondary structure prediction and validation of the construct

The secondary structure composition of the insilico vaccine construct retrieved from PSIPRED workbench is given in Fig. 2a. Based on the PSIPRED workbench illustration, the vaccine construct consists of alpha helices, strands and transmembrane domains. No disordered proteins were observed. The graphical representation of the percentage composition of the secondary structure of the multi-epitope vaccine construct retrieved from GOR4 server is given in Fig. 2b. The secondary structure comprises of 7.04% of alpha helices, 24.09% of extended strands (beta strands) and 68.87% of random coils. The cartoon representation of the secondary structure of each amino acid residue in vaccine construct sequence retrieved from PSIPRED workbench is given in Fig. 3.

The presence of alpha helices and beta strands, although in smaller proportions, suggests that the vaccine construct has specific regions that are likely to be more structurally stable and might play key roles in maintaining the overall structure or in specific functional sites. Natively unfolded protein regions (random coils) and alpha-helices are significant structural antigens. These structures can maintain their native configurations, allowing them to be recognized by antibodies produced in response to infection[78]. The dominance of random coils implies that the vaccine construct has a high degree of structural flexibility, which can be advantageous for interacting with different antigens or receptors. Random coils are often associated with regions of proteins that

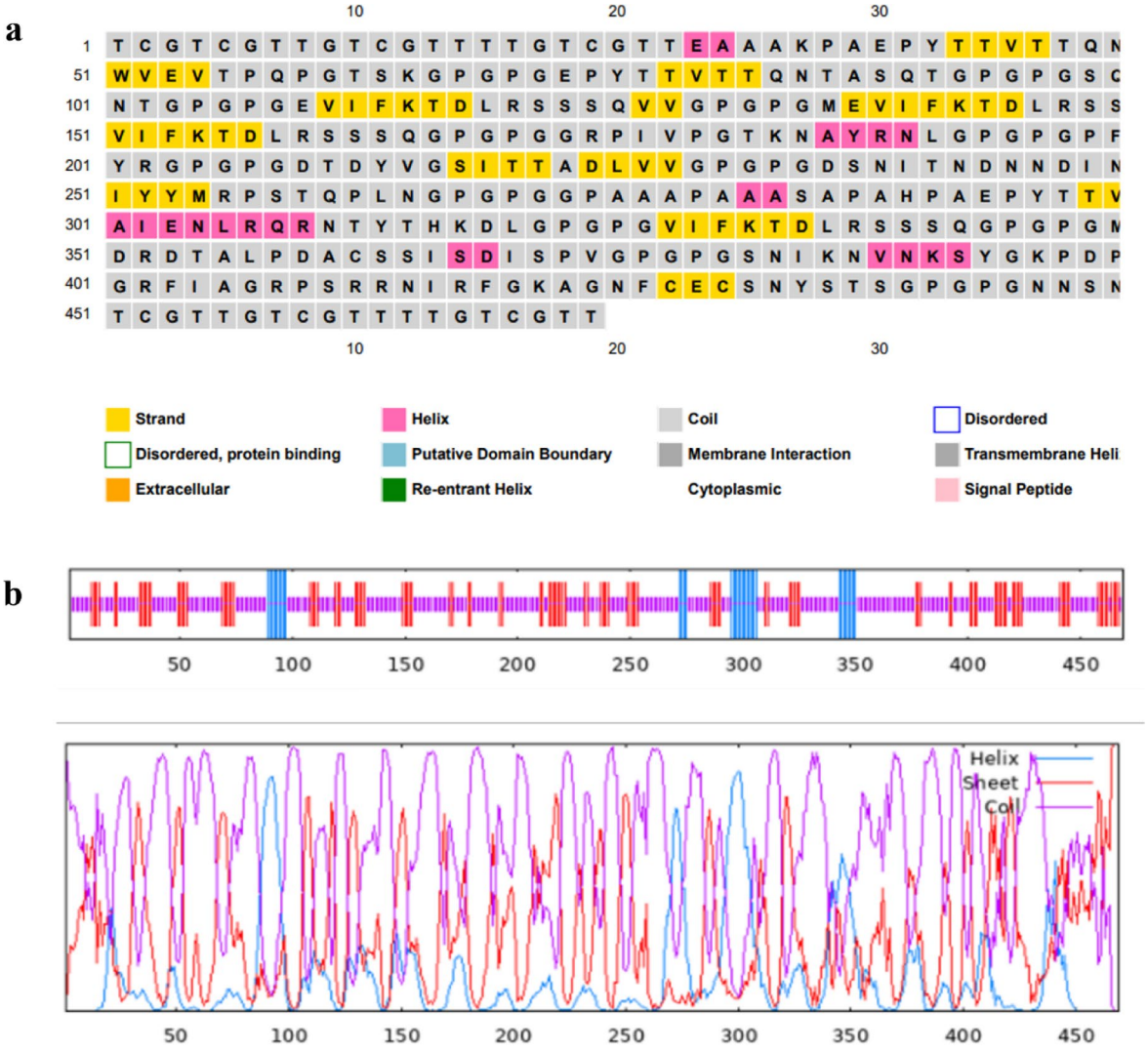

Fig. 2. (**a**) The illustration of the secondary structure of the secondary structure of the vaccine construct. The vaccine construct consists of strands, helices and transmembrane domains. (**b**) Graphical representation of the secondary structure of the vaccine construct. The secondary structure components present include - Alpha helix (blue), beta – sheets (red) and random coils (purple).

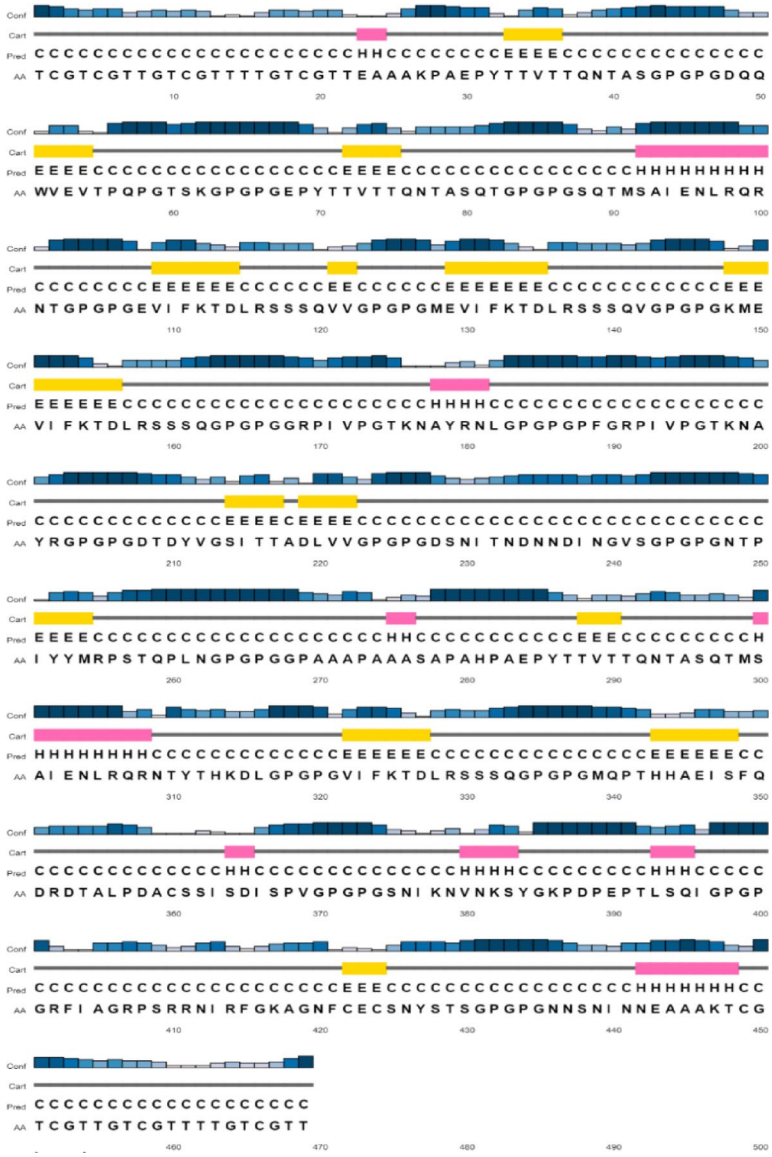

Fig. 3. Cartoon representation of the secondary structure of the vaccine construct. Conf represents the confidence of prediction. Cart is a 3-state assignment cartoon which is the graphical representation for each amino acid residue in the secondary structure. Pred is predicted secondary structure classification for each amino acid residue in the protein sequence - helix(H), bets-strand (E) and coil (C). Yellow, pink and grey bars represent beta strand, alpha-helix and random coils respectively.

are more accessible to antibodies, which can be beneficial for a vaccine as it might enhance the immune system's ability to recognize and respond to the antigen[79]. No beta turns, bend regions, beta bridges, ambiguous and other states. The absence of these elements suggests that the secondary structure of the vaccine construct is relatively straightforward, predominantly comprising alpha helices, extended strands, and random coils without more complex or less common structural motifs. The clear categorization into alpha helices, beta strands, and random coils with no ambiguous or less common structures might indicate a high confidence in the prediction. While beta turns and bend regions often play roles in the flexibility and functionality of proteins, their absence suggests that this particular protein might rely more on the larger and more defined secondary structures (helices and strands) and random coils for its functional properties[80,81].

Tertiary structure prediction and validation of the construct

The tertiary structure modelled with the AlphaFold3 server and further refined using the Galaxy Refine and viewed with ChimeraX is provided in Fig. 4.

The quality of the protein structure was assessed using ERRAT (Empirical R-factor for Assessment of Templates), a method that evaluates the agreement between the structural parameters of the model and those of highly refined structures of similar size. The ERRAT score obtained was 72.5173, indicating that 72.52% of the residues in the protein structure are located in regions with good agreement with known high-resolution

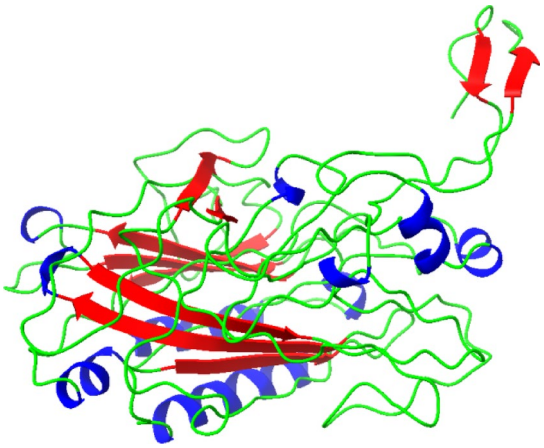

Fig. 4. Tertiary structure of the ASFV multi-epitope vaccine construct. The alpha helix (blue), beta sheet (red) and random coil (green) are given.

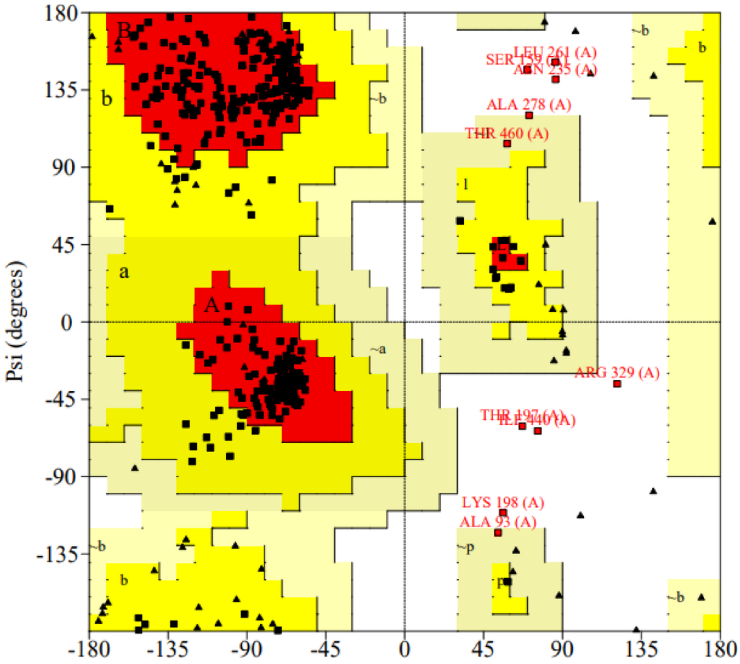

Fig. 5. The Ramachandran plot of the vaccine construct. It depicts the amino acid residues located in most favoured (red), additionally allowed (yellow), generously allowed (peach) and disallowed (white) regions.

structures. This score ranges from 0 to 100, where higher scores indicate better agreement with expected values from high-quality structures. Generally, structures with ERRAT scores above 50 are considered to have acceptable quality[82]. This suggests that the overall quality of the model is reasonable, with the majority of residues adopting conformations typical of well-resolved protein structures.

The Ramachandran plot is crucial for visualizing, analyzing and validating polypeptide chain conformations in proteins through the distribution of backbone dihedral angles (phi (φ) and psi (ψ)), that form the protein backbone. Additionally, it offers insights into amino acid conformational preferences, aiding in the understanding of protein folding and stability. The phi and psi distributions of the amino acid residues (excluding glycine and proline) are presented in the Ramachandran plot (Fig. 5). The vaccine construct has 85.9% of residues in the highly favoured region, 11.1% of residues in the additionally allowed region and 0.6% in the generously allowed region. The higher the number of residues in the favourable region, the higher the quality of the protein model[83]. Hence our construct is a well-validated and stable protein structure suggesting that the majority of the protein's backbone dihedral angles (phi (φ) and psi (ψ)) are in conformations that are sterically allowed and energetically favourable, reflecting proper folding and stability crucial for its function as a vaccine[84]. Additionally allowed regions indicate slightly less favourable yet acceptable conformations for proteins and generously allowed regions include residues in the less common but still permissible conformations that but will not create major

structural issues. The residues in the disallowed region were 2.4%, indicating minor structural issues and regions of flexibility arising due to Van der Waals clashes[85].

Molecular docking

The vaccine construct was successfully docked with SLA-1 0401 using the protein-protein docking mode of the ClusPro server. The mode uses Piper, a Fast- Fourier Transform based rigid docking program. This FFT program provides 10^3 positions out of the 10^9 positions of the ligand with respect to the receptor based on 9 angstrom C-alpha RMSD radius, which implies identifying a ligand position surrounded by the highest number of neighbouring atoms within a 9-angstrom distance. This position then serves as the cluster center, with its surrounding atoms designated as cluster members[86]. The server provides a summary table with a list of models generated and their corresponding cluster size and energy. Based on the criteria mentioned, the model with cluster of 67 members with center energy of -864.8 and lowest energy of -1146.5 was selected. The docked model and the amino acid residue interactions were viewed using PyMOL (Fig. 6a,b).

Molecular dynamics simulations and normal mode analysis

The molecular dynamics predictions from PRODIGY webserver relate to the binding strength and stability of a molecular interaction. The Predicted binding affinity of -6.7 kcal/mol was obtained. A negative value indicates a stronger binding interaction. The dissociation constant (Kd) is a measure of how tightly a ligand binds to a particular receptor or protein. A lower Kd value indicates a stronger binding affinity. Likewise, the docked model has a Kd value of 2.0e-05 M (20 nanomolar), which indicates a stronger binding affinity. This means at equilibrium, only a small concentration of the ligand is needed to bind half of the receptor sites. These predictions suggest that the vaccine construct and receptor form a strong and stable binding complex, supported by the negative binding affinity and the low dissociation constant.

The MD simulations of the Maestro protein were conducted under the NPT ensemble at 300 K and 1 bar pressure for 100 ns. The stability of the protein structure was monitored throughout the simulation, with the RMSD of atomic positions remaining relatively stable, indicating no significant conformational changes. The interactions between the protein and its surrounding environment were analyzed using the Simulation Interaction Diagram tool, revealing key binding interactions and structural features critical for its function. Initially, the RMSD (Root Mean Square Deviation) of the protein's atomic positions fluctuated around 7 Å, indicating some initial structural adjustment. However, after equilibration, the RMSD stabilized within a range of approximately 4 to 5 Å, reflecting a stable conformation throughout the simulation. The Root Mean Square Fluctuation (RMSF) of the protein ranged from 1.2 to 3.6 Å, with minor fluctuations observed in specific regions of the protein. These fluctuations are typical in flexible regions, while the core structure remained relatively stable. The results suggest that the Maestro protein maintains its overall stability while exhibiting localized flexibility in certain areas. The root mean square deviation (RMSD) of the protein–vaccine complex initially exhibited fluctuations between 6 and 12 Å, reflecting conformational adjustments during the equilibration phase. Around 40 ns, the RMSD stabilized, suggesting the attainment of a stable binding conformation. Mild fluctuations were observed beyond 40 ns, ranging between 15 and 24 Å, which may indicate transient conformational rearrangements without compromising the overall stability of the complex (Fig. 7a,b). Root mean square fluctuation (RMSF) analysis revealed consistent stability across the majority of residues, with fluctuations ranging between 4 and 12 Å. Notably, elevated flexibility was observed in the region starting from residue 800, where fluctuations increased to a range of 12 to 24 Å. This may correspond to a loop or terminal region contributing to the dynamic nature

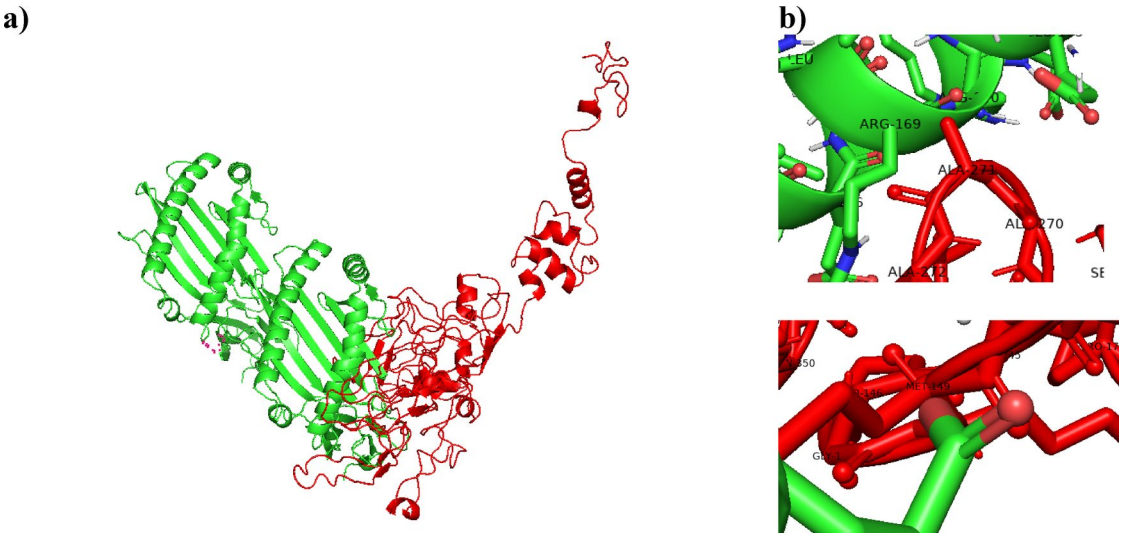

Fig. 6. (**a**) The multi-epitope vaccine construct (red) docked with SLA-1 0401 (green); (**b**) Manual zoom of the interactions between the amino acid residues of the ligand and receptor.

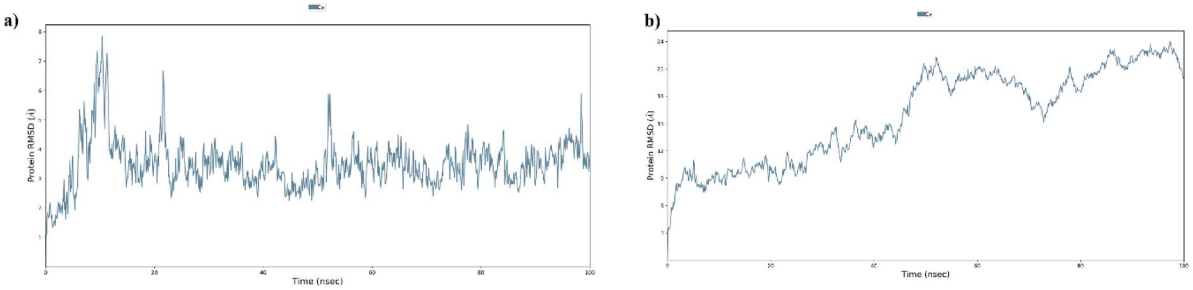

Fig. 7. Time evolution of the RMSD of the (**a**) SLA-1 0401 receptor and (**b**) complex of the vaccine construct and receptor.

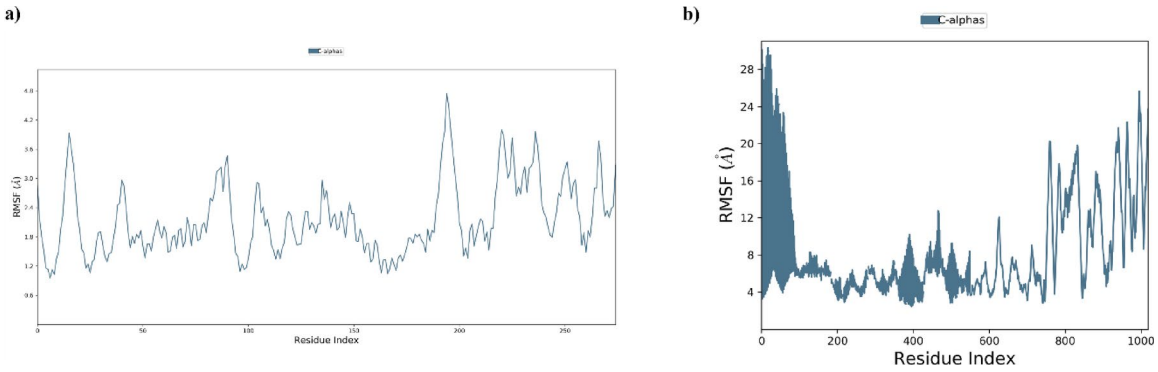

Fig. 8. RMSF plots (**a**) SLA-1 0401 receptor and (**b**) complex of the vaccine construct and receptor.

of the complex (Fig. 8a,b). These findings demonstrate that the interface between the vaccine construct and the SLA-04:01 receptor remains stable under dynamic conditions.

iMODS webserver uses normal mode analysis to study the dynamics of the docked complex. The main-chain deformability graph sums atomic displacements across all modes per residue to highlight deformable protein regions (Fig. 9a). The B-factor graph indicates relative atomic displacement amplitudes around equilibrium, showing the relationship between the mobility of the docked complex and PDB scores (average RMSDs). For deformity and B factor graph, the high peaks represent flexible regions and low peaks represents rigid regions. Based on the two graphs, the docked complex has both flexible and rigid regions suggesting a balanced structural adaptation (Fig. 9b). The eigenvalues graph indicates stiffness with lower values signifying easier alpha carbon deformations. For the docking complexes, eigenvalues were found to be 6.285800×10^{-6} (Fig. 9c). Eigenvalues represent the stiffness and lower eigenvalues can indicate flexibility in critical regions, potentially aiding in antigen presentation or binding interactions. Based on the eigen value, our docked complex is stable. The variance graph highlights the contribution of each normal mode to the complex's motion, with higher variance modes contributing more significantly to structural dynamics (Fig. 9d). The covariance matrix demonstrates correlated (red), uncorrelated (white), or anti-correlated (blue) atomic movements within the complex (Fig. 9e). Covariance maps indicate how pairs of residues experience these motion dynamics. The elastic network model illustrates relationships of atoms, with dot colors indicating stiffness; darker dots indicating stiffness while lighter dots indicate flexibility. Our complex has a darker grey model, emphasizing stability (Fig. 9f). Altogether, our docked complex of SLA-1 0401 and multi-epitope ASFV vaccine is stable based on iMODS simulation[63,66].

Immune response profile of multi-epitope ASF vaccine

The immunological simulation of the multi-epitope ASF vaccine was assessed using the C-ImmSim tool, which also predicted the ability of the epitopes to induce both humoral and cell-mediated adaptive immunity. This investigation elucidated the immunological interactions between the epitopes and their specific targets. According to the simulation analysis, the antigen level peaked at approximately 7×10^5 antigen count mL^{-1} and then stabilized to a baseline by day 5 post-vaccination (Fig. 10a). The results from the C-ImmSim server indicated an increase in secondary immune response generation, mirroring the actual immunological response. Notably, immunoglobulin production, including IgM and IgG, was observed, with the combined amount of IgM and IgG reaching around 2.1×10^4 antigen count mL^{-1} on an arbitrary scale by the 15th day after antigen exposure (Fig. 10a). The B-cell population of isotype IgM was elevated to around 500 cells per mm^3 and continued to rise over 30 days post-exposure. Memory B-cells reached their peak around 6 days post-exposure and remained elevated for a month. Among the different B-cell states, the active isotype persisted longer than others (Fig. 10b–

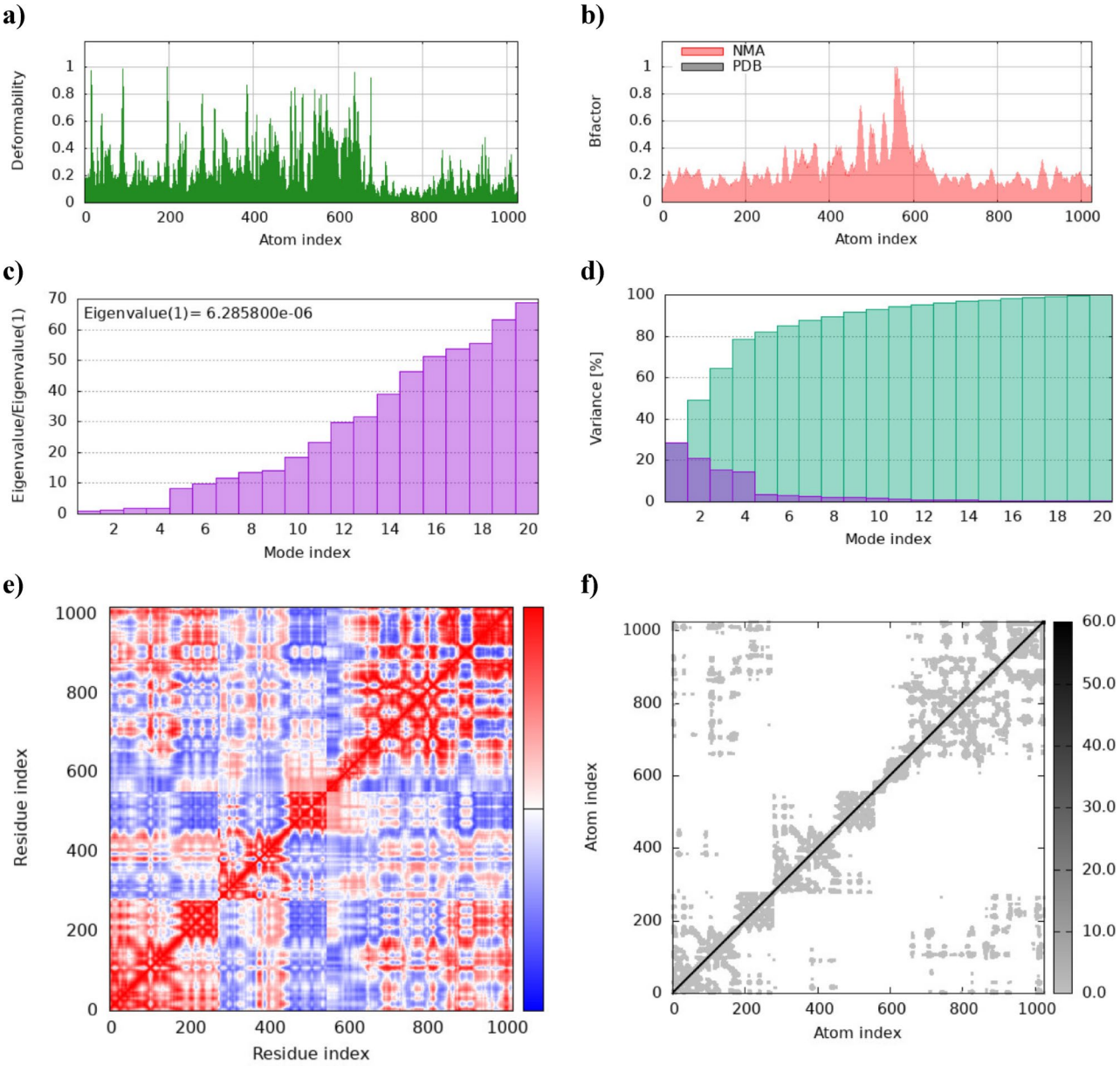

Fig. 9. NMA of the complex using iMODS. (**a**) Main-chain deformability graph; (**b**) B-factor graph; (**c**) Eigenvalues graph; (**d**) Variance graph; (**e**) Covariance matrix; (**f**) Elastic network.

d). Additionally, there were notable increases in plasma B cells, helper T cells (HTLs), cytotoxic T cells (CTLs), and natural killer (NK) cells, indicating a robust immune response with high potency, immunological memory, and efficient antigen clearance from the host (Fig. 10e–j). DC can present antigenic peptides on both MHC class-I and class-II molecules. Also, macrophages help in antigenic presentation on MHC class-II molecules. The rise in dendritic cells and macrophages indicated enhanced antigen presentation by APCs, while the activation of helper T cells underscores the vaccine effective adaptive immunity (Fig. 10k,l). There is an increase in count of epithelial cells that are broken down to active, virus-infected and presenting on class-I MHC molecule (Fig. 10m). Furthermore, a significant increase in interferon-gamma (IFN-γ), a cytokine involved in both innate and adaptive immunity, was observed, peaking between days 11 and 16. Other simulated cytokines, including TGF-β, IL-10, and IL-12, were also detected (Fig. 10n). The substantial production of APCs, cytokines, active B cells, and T cells highlighted the promising characteristics of the vaccine, suggesting that the multi-epitope in silico ASF vaccine elicited strong immunogenic reactions upon administration to the host.

Codon optimization

The Vector Builder optimizes the sequence of the input vaccine construct to enhance its expression in the selected host organism, *Sus scrofa*. It calculates key metrics such as the Codon Adaptation Index (CAI) and the GC content of the optimized sequence, resulting in values of 0.85 and 64.26%, respectively. These metrics are

critical for determining expression efficiency in the host organism. A CAI value above 0.8 and a GC content ranging from 30 to 70% are typically preferred for achieving robust expression. Our optimized construct falls well within these favourable ranges, indicating promising potential for enhanced expression in the chosen host organism[87]. This optimization process ensures that the DNA sequence is tailored to match the codon usage preferences of *Sus scrofa (pig)*, thereby maximizing the likelihood of successful protein expression.

Insilico cloning of the construct

The adapted vaccine sequence was successfully inserted into the pVAX1-eGFP vector using the NovoBuilder tool (Fig. 11a,b). pVAX1-EGFP is mammalian expression vector tagged with a reporter gene - Enhanced Green Fluorescent Protein (EGFP). The construct comprises of a CMV (cytomegalovirus) promoter, multiple cloning site, antibiotic (kanamycin or neomycin) resistance genes and a polyadenylation signal. The cloning process involved the precise insertion of the sequence between the EcoRI and BamHI restriction sites. The insert size is 1410 bp.

Discussion

The advent of immunoinformatics has revolutionized vaccine design, particularly in the development of multi-epitope vaccines. Traditional vaccine development is often slow and can face challenges such as adverse reactions. Multi-epitope vaccines, however, target multiple antigenic sites of a pathogen, eliciting a broad and robust immune response and reducing the likelihood of immune escape. Immunoinformatics leverages computational tools to identify and analyze potential epitopes, which allows researchers to design highly specific and effective vaccines. By predicting B-cell and T-cell epitopes, assessing their immunogenicity, optimizing their combination into a single construct, followed by further analyses, multi-epitope vaccines offer enhanced efficacy and safety.

In the present study, immunoinformatics was used to identify and analyse epitopes to design a multi-epitope vaccine candidate for ASFV. Based on previous works, conserved proteins that play crucial role in ASFV infection and replication were selected for selection of target epitopes, as conserved proteins provide broader range of protection against different strains of the pathogen[36,88–91]. The vaccine construct composed of 12 HTL epitopes and 7 BL epitopes of the conserved proteins. The HTL epitopes were scrutinized based on the score and rank from MHC II Binding Prediction set - NetMHCIIpan 4.1 EL of the IEDB server and the BL epitopes based on threshold value from BepiPred Linear Epitope 2.0 (BLE) tool of IEDB webserver. Antigenic (antigenic score > 0.5) and non-allergenic (non-allergen score > 0.5) epitopes that were reconfirmed to be conserved were finalized for vaccine construct, expecting a heightened immune response. Amongst several webservers available for epitope prediction, the tools from IEDB were used based on the high result accuracy obtained in a previous study[92].

The GPGPG linker was used to connect each epitope and an EAAAK linker at the first and last epitope to connect it with the adjuvant CpG-ODN 2007. CpG-ODN was selected based on previous research that showed that this oligonucleotide as a vaccine adjuvant induced a rapid and protective toxin-neutralizing Ab response in guinea pigs[93]. Another study on PRRSV vaccine using CpG-ODN 2007 as an adjuvant also has promising results[94]. This adjuvant activates TLR9 receptor that enhances antigen presentation by macrophages thereby stimulating the production of pro-inflammatory cytokines and interferons, eliciting a strong adaptive immune response[95]. With these abilities of each component of construct, the multi-epitope vaccine built looks promising. The vaccine construct was rechecked for antigenicity, allergenicity and cross reactivity. The vaccine construct was non-allergenic with a TSI score of 0.83 and antigenic with a prediction score of 0.6421. The observed antigenicity scores are better than that of previous multi-epitope vaccine constructs designed for ASFV[31,33]. No cross-reactivity was observed confirming no unwanted immune reactions[96].

The vaccine construct was made of 469 amino acids with a molecular weight of 47343.02 Da. Proteins with a molecular weight under 110 kDa are often considered promising candidates for vaccine development owing to their solubility and the ease of purification[97]. Based on the instability index, our construct is stable. The SOLpro results predict 90% solubility. Based on the physicochemical parameters analysed, the designed multi-epitope ASFV vaccine is a stable and soluble vaccine construct, which is crucial for vaccines[98].

The secondary structure composition of a vaccine, with alpha helices, beta strands, and random coils, plays a crucial role in its immune response efficacy. The tertiary structure was modelled and refined and analysed. Based on the ERRAT scores, the vaccine construct has acceptable quality. Based on Ramachandran Plot, 85.9% of residues are in the favourable region denoting high quality of the model.

The docking of the vaccine construct comprising of B-cell and Helper T-cell epitopes with SLA-1 0401 with a binding affinity of -6.7 kcal/mol indicates that the epitopes have high binding affinity for SLA-1*0401 and can be effectively presented by the swine MHC class I molecule. This recognition is essential for eliciting a robust immune response, involving both antibody production by B cells and activation of cytotoxic T cells. The Kd value of 20 nanomolar indicates high affinity that corresponds to tight binding interactions, which are essential for the stable presentation of antigens to T cells.

MD simulations were conducted to evaluate the structural integrity and interaction dynamics of a designed multi-epitope vaccine construct in complex with the SLA-04:01 immune receptor. The RMSD profile of the SLA-04:01–vaccine complex revealed initial fluctuations between 6 and 12 Å, followed by stabilization around 40 ns. After equilibration, the complex maintained structural integrity with mild fluctuations between 15 and 24 Å, suggesting a dynamic yet stable interaction, likely due to conformational adjustments within the SLA-04:01 binding groove. These RMSD values are higher than those reported by Fagbohun et al., where the SLA-1–vaccine complex stabilized at ~ 1.1 nm within 4 ns, possibly reflecting increased flexibility or induced-fit interactions in the current construct[70].

RMSF analysis indicated notable flexibility beyond residue 800, likely corresponding to linker or terminal regions designed for epitope accessibility. Compared to Nguyen et al., who reported average RMSF values of

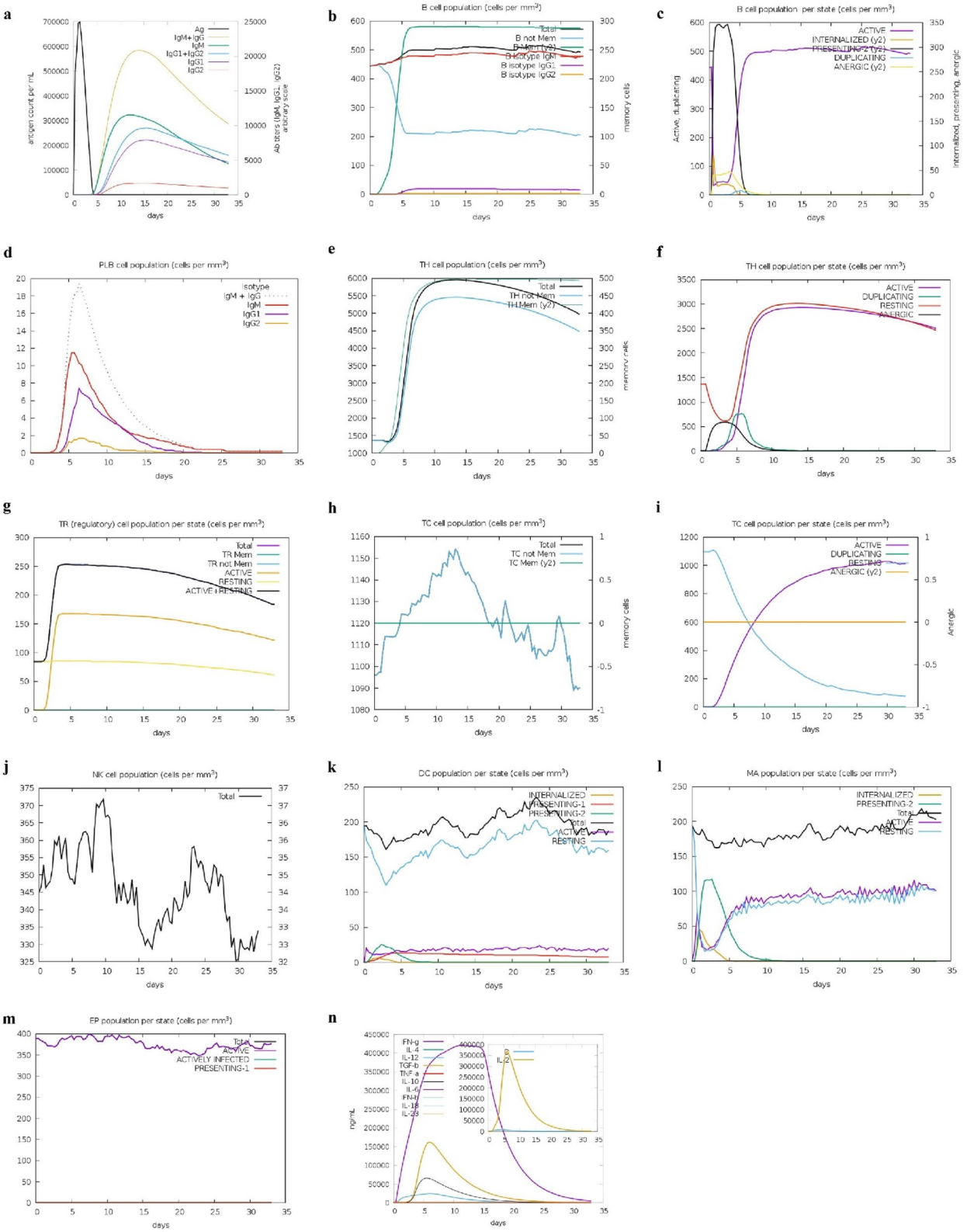

0.60 ± 0.27 nm for a TLR5–vaccine complex, the current construct exhibited broader fluctuations (4–24 Å), which may enhance antigen presentation and receptor engagement[33].

Unlike the Rg and density-based assessments used by Fagbohun et al., the current study utilized trajectory and interaction mapping from the Desmond package, revealing stable post-equilibration contact profiles and minimal structural deviation[70]. Overall, the results demonstrate that the designed multi-epitope vaccine construct maintains a stable yet flexible conformation when bound to SLA-04:01, highlighting its immunogenic promise and structural robustness for further vaccine development.

◀**Fig. 10**. (**a**) Immunoglobulin production (coloured peak) in response to antigen (black peak); (**b**) B lymphocytes: total count, memory cells, and sub-divided in isotypes IgM, IgG1 and IgG2; (**c**) B Lymphocyte population per entity state; (**d**) Plasma B lymphocytes count sub-divided per isotype (IgM, IgG1 and IgG2); (**e**) CD4 T-helper lymphocytes and memory count; (**f**) CD4 T-helper lymphocytes count sub-divided per entity-state; (**g**) CD4 T-regulatory lymphocytes count comprising of total, memory and per entity state counts; (**h**) CD8 T-cytotoxic lymphocytes count showing total and memory; (**i**) CD8 T-cytotoxic lymphocytes count per entity-state; (**j**) Natural Killer cells total count; (**k**) Dendritic cells count per state of antigen presentation; (**l**) Macrophages: Total count, internalized, presenting on MHC class-II, active and resting macrophages; (**m**) Epithelial cells: Total count broken down to active, virus-infected and presenting on class-I MHC molecule; (**n**) Cytokines: Concentration of cytokines and interleukins with IL2 level and Simpson index (D) in the inset plot.

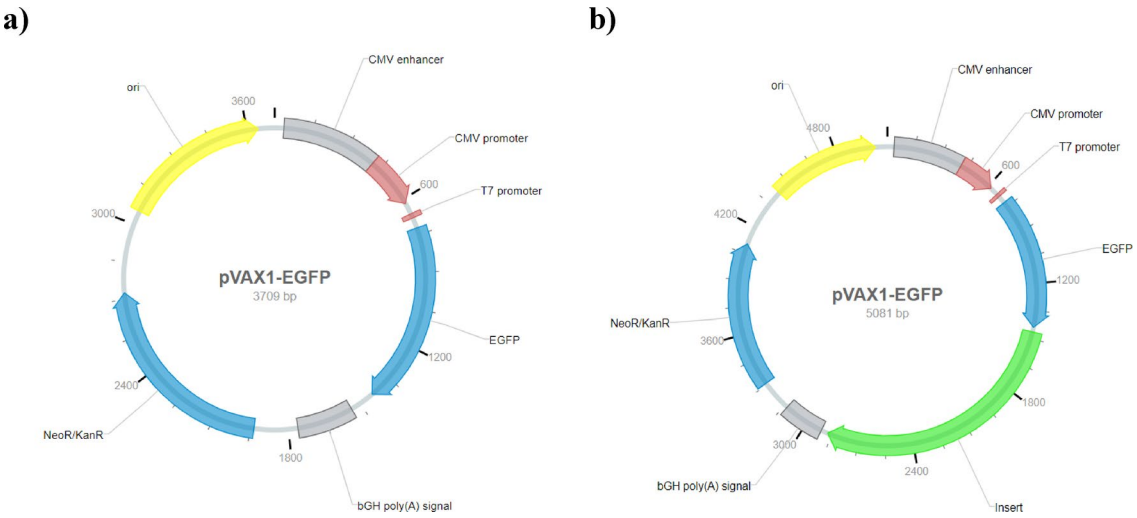

Fig. 11. (**a**) pVAX1-EGFP plasmid with insert. (**b**) pVAX1-EGFP with insert (green) between EcoRI and XbaI restriction sites.

Based on the iMODS simulation, the combination of balanced flexible and rigid regions, favourable eigenvalue, and a predominantly stiff elastic network all point to a highly stable docked complex[51]. Overall, the docking and dynamics simulation result suggests that the vaccine construct has the potential to be effective in swine, as it can be effectively presented and engage the immune system via both humoral and cellular pathways. The inclusion of both B cell and HTL epitopes ensures a comprehensive immune response, which is beneficial for long-term immunity and memory formation[99,100].

The simulation analysis of the multi-epitope ASFV vaccine revealed a dynamic and robust immune response post-vaccination, with antigen levels peaking at 7×10^5 antigen count mL^{-1} and stabilizing by day 5. Enhanced antigen presentation was indicated by increased dendritic cells and macrophages, which led to the activation of helper T cells and cytotoxic T cells. The vaccine elicited a strong humoral response, with IgM and IgG levels reaching 2.1×10^4 antigen count mL^{-1} by day 15, and a sustained elevation in B-cell populations, particularly memory B cells. Cellular immunity was marked by rises in plasma B cells, HTLs, CTLs, and NK cells, emphasizing a coordinated defense strategy. Epithelial cells presented antigens on MHC class I molecules, facilitating infected cell clearance. Significant cytokine production, especially IFN-γ peaking between days 11 and 16, further underscored the vaccine's efficacy in enhancing both innate and adaptive immunity.

The optimized multi-epitope ASFV vaccine sequence shows a Codon Adaptation Index (CAI) of 0.85 and a GC content of 64.26%. A CAI of 0.85 indicates efficient codon usage for expression in Sus scrofa, ensuring robust antigen production. The GC content of 64.26% supports gene stability and efficient expression. These metrics confirm that the vaccine construct is likely to be effectively expressed in the host, enhancing its potential efficacy against ASFV.

The field of in silico-based vaccine development for ASFV is rapidly evolving, yet remains relatively unexplored, with limited prior publications available for reference. However, some studies have employed multi-epitope vaccine design strategies for ASFV and other viral pathogens. Buan et al. constructed a multi-epitope vaccine using B-cell (BL), Helper T-cell (HTL), and Cytotoxic T-cell (CTL) epitopes from six different ASFV genes, achieving an antigenicity score of 0.5344[31]. In contrast, our vaccine construct, designed using epitopes from only four ASFV genes and incorporating only BL and HTL epitopes, demonstrated a higher antigenicity score of 0.6421. Additionally, unlike their study, we performed molecular dynamics simulations, further enhancing the reliability and structural stability of our construct. Though their CAI-value (0.9361) was higher than ours (0.85) ensuring better expression in *Sus scrofa*, our GC content (64.26%) is higher than theirs (54.94%) ensuring greater mRNA stability and efficient expression, which can be advantageous for sustained antigen production.

Nguyen et al. also utilized epitopes from six ASFV genes, with a similar approach in selecting only BL and HTL epitopes, and no CTL epitopes[33]. However, a key distinction lies in the structural design of our vaccine construct, particularly in the placement of GPGPG linkers. While Nguyen et al. positioned GPGPG linkers between entire groups of HTL and BL epitopes, our study placed linkers between each individual epitope, improving epitope presentation, flexibility, and stability[34]. Fagbohun et al. also developed an immunoinformatics-based multi-epitope vaccine against ASFV, utilizing epitopes from three target genes—p72, CD2 homologue (CD2v), and C-type lectin[70]. While their methodology closely aligns with ours, they additionally incorporated interferon-gamma (IFN-γ) inducing epitopes to enhance immune activation. In terms of physicochemical properties, their construct demonstrated better stability and solubility compared to ours. Their vaccine also achieved a VaxiJen v.2.0 antigenicity score of 0.6782, which is slightly higher than our score. However, this was assessed at a threshold of 0.4, whereas our antigenicity score of 0.6421 was determined at a more stringent threshold (≥ 0.5), making direct comparisons challenging. A key distinction between the two approaches is the choice of adjuvants. Fagbohun et al. employed Sus scrofa β-defensin at the N-terminal to enhance structural rigidity and reduce potential interference in adjuvant-receptor interactions[72]. Additionally, they used a TAT signal at the C-terminal to improve intracellular delivery. In contrast, our study utilized CpG ODN 2007, a TLR9 agonist, which directly stimulates the innate immune system, leading to a more robust adaptive immune response, including enhanced T-cell activation and antibody production. These variations in design strategies highlight different approaches to optimizing vaccine efficacy. Other multi-epitope vaccine studies against ASFV included Chen et al. and Ros-Lucas et al., dealt majorly with the optimization of the epitope selection process. While the former used Pareto front-based ASFV screening method PFAS to identify promising epitopes for designing multi-epitope vaccines, the latter used an in-house pipeline based on publicly available immunoinformatic tools to identify epitopes of interest for a prospective vaccine ensemble[71,101]. These comparisons highlight the advancements and optimizations in our multi-epitope vaccine design, reinforcing its potential effectiveness and reliability for further experimental validation.

The multi-epitope ASFV vaccine construct incorporates key proteins p72, p30, p54, and CD2v, targeting various critical aspects of the immune response for enhanced efficacy. p72, the major capsid protein, is highly immunogenic and crucial for virus assembly, eliciting strong NAbs and inducing IFN-γ, which enhances macrophage activation and antigen presentation[102]. p30, expressed early during infection, facilitates viral entry and replication, targeting cellular receptors and inducing cytokines such as IL-12 and IFN-γ, essential for activating NK cells and CTLs[103]. p54, a structural protein involved in virus assembly and budding, targets cellular components crucial for virus integrity and induces antiviral cytokines IFN-α and IFN-β[104]. CD2v, a viral homologue of the host's CD2 protein, interferes with immune cell signalling to evade immune responses; its inclusion in the vaccine helps neutralize this evasion, and it induces IL-10, modulating the immune response[46,105]. This combination of proteins ensures a comprehensive and robust immune response, addressing multiple stages of the viral life cycle and various viral components. The vaccine promotes early intervention through p30[106], sustained immune activity through p72 and p54[107], and counteracts viral immune evasion via CD2v[108]. Enhanced cytokine production, particularly IFN-γ, IL-12, IFN-α, IFN-β, and IL-10, further underscores the vaccine's potential to stimulate both innate and adaptive immunity effectively.

Despite these promising results, the current study has some limitations that needs to be acknowledged. The vaccine construct was designed entirely through computational analyses, and in vitro and in vivo validation is required to confirm its efficacy and safety in the real-world conditions that shall involve complex interplay of host factors. Additionally, while the selected epitopes are conserved among ASFV strains, emerging viral mutations could impact vaccine effectiveness over time. Another limitation is the reliance on predictive models for antigenicity and immunogenicity, which may not fully replicate real-world immune responses. The study also does not evaluate potential challenges in large-scale vaccine production, such as stability during formulation, storage conditions, or potential degradation of the vaccine construct over time. Future work should focus on experimental validation, including cell culture-based assays and animal trials, to assess immunogenicity, stability, and potential protective efficacy.

By ensuring robust antigen presentation and neutralization, this multi-epitope vaccine offers superior protection against ASFV compared to vaccines targeting fewer or less critical viral proteins based on immunoinformatics approach.

Conclusion

Bioinformatics, particularly immunoinformatics, plays a pivotal role in predicting immunogenic epitopes, essential for designing effective vaccines. The multi-epitope and multi-antigenic ASF vaccine, constructed using predicted B-cell and helper T-cell epitopes from conserved antigens (p30, p54, p72, and CD2v), has demonstrated antigenicity, immunogenicity, and non-allergenicity—key parameters for vaccine design. The physicochemical profile and validation of the 2D and 3D structures of the vaccine construct showed positive results. Molecular docking studies confirmed the strong binding affinity of the final construct with target receptor. Immune simulation revealed that T-helper lymphocytes triggered cytokine release, enhancing the cytotoxic activity of CTLs and NK cells. Additionally, the simulations indicated that the ASF vaccine could induce a pertinent immune response by triggering both humoral and cell-mediated immunity against ASFV. The use of various in silico tools provided promising results, representing a crucial first step in designing effective and safe ASF vaccines, reducing labour, cost, and time. The developed multi-epitope ASFV vaccine appears promising and warrants further in vitro and in vivo screening to confirm its protective efficacy against ASF infection under natural conditions.

Data availability

All data analyzed during this study are included in this published article. The raw data are available from the corresponding author upon reasonable request.

Received: 27 November 2024; Accepted: 29 April 2025
Published online: 08 May 2025

References

1. Wang, G., Xie, M., Wu, W. & Chen, Z. Structures and functional diversities of ASFV proteins. *Viruses* **13** https://doi.org/10.3390/v13112124 (2021).
2. Salguero, F. J. Comparative pathology and pathogenesis of African swine fever infection in swine. *Front. Veterinary Sci.* **7**, 282 (2020).
3. Yang, S. et al. Structure and function of African swine fever virus proteins: current Understanding. *Front. Microbiol.* **14**, 1043129. https://doi.org/10.3389/fmicb.2023.1043129 (2023).
4. Wang, T., Luo, R., Sun, Y. & Qiu, H. J. Current efforts towards safe and effective live attenuated vaccines against African swine fever: challenges and prospects. *Infect. Dis. Poverty*. **10**, 137. https://doi.org/10.1186/s40249-021-00920-6 (2021).
5. Wang, Y. et al. Structure of African swine fever virus and associated molecular mechanisms underlying infection and immunosuppression: A review. *Front. Immunol.* **12**, 715582. https://doi.org/10.3389/fimmu.2021.715582 (2021).
6. Gaudreault, N. N., Madden, D. W., Wilson, W. C., Trujillo, J. D. & Richt, J. A. African swine fever virus: an emerging DNA arbovirus. *Front. Vet. Sci.* **7**, 215. https://doi.org/10.3389/fvets.2020.00215 (2020).
7. Dinhobl, M. et al. Reclassification of ASFV into 7 biotypes using unsupervised machine learning. *Viruses* **16** https://doi.org/10.3390/v16010067 (2023).
8. Onoja, A., Ifeorah, I., Jolaoso, M. & Onoja, I. Detection of African swine fever virus genotype II in domestic pigs during a hemorrhagic fever outbreak in Ogun State, Nigeria. *Nigerian Veterinary J.* **43**, 33–41 (2023).
9. Obanda, V. et al. Epidemiology and ecology of the sylvatic cycle of African swine fever virus in Kenya. *Virus Res.* **348**, 199434 (2024).
10. Ruedas-Torres, I., Thi to Nga, B. & Salguero, F. J. Pathogenicity and virulence of African swine fever virus. *Virulence* **15**, 2375550 (2024).
11. Venkateswaran, D. et al. Comprehensive characterization of the genetic landscape of African swine fever virus: insights into infection dynamics, Immunomodulation, virulence and genes with unknown function. *Animals* **14** https://doi.org/10.3390/ani14152187 (2024).
12. Chandana, M. S. et al. Recent progress and major gaps in the vaccine development for African swine fever. *Braz J. Microbiol.* https://doi.org/10.1007/s42770-024-01264-7 (2024).
13. Urbano, A. C. & Ferreira, F. African swine fever control and prevention: an update on vaccine development. *Emerg. Microbes Infect.* **11**, 2021–2033. https://doi.org/10.1080/22221751.2022.2108342 (2022).
14. Pikalo, J. et al. Vaccination with a gamma irradiation-inactivated African swine fever virus is safe but does not protect against a challenge. *Front. Immunol.* **13**, 832264 (2022).
15. Blome, S., Gabriel, C. & Beer, M. Modern adjuvants do not enhance the efficacy of an inactivated African swine fever virus vaccine Preparation. *Vaccine* **32**, 3879–3882 (2014).
16. Lacasta, A. et al. Live attenuated African swine fever viruses as ideal tools to dissect the mechanisms involved in viral pathogenesis and immune protection. *Vet. Res.* **46**, 135. https://doi.org/10.1186/s13567-015-0275-z (2015).
17. Zhang, H. et al. Vaccines for African swine fever: an update. *Front. Microbiol.* **14**, 1139494. https://doi.org/10.3389/fmicb.2023.1139494 (2023).
18. Krug, P. W. et al. The progressive adaptation of a Georgian isolate of African swine fever virus to Vero cells leads to a gradual Attenuation of virulence in swine corresponding to major modifications of the viral genome. *J. Virol.* **89**, 2324–2332 (2015).
19. Wang, T., Luo, R., Sun, Y. & Qiu, H. J. Current efforts towards safe and effective live attenuated vaccines against African swine fever: challenges and prospects. *Infect. Dis. Poverty*. **10**, 83–89 (2021).
20. Zhang, J. et al. Deletion of the L7L-L11L genes attenuates ASFV and induces protection against homologous challenge. *Viruses* **13**, 255 (2021).
21. Lim, J. W. et al. Advanced strategies for developing vaccines and diagnostic tools for African swine fever. *Viruses* **15** https://doi.org/10.3390/v15112169 (2023).
22. Zhang, G. et al. Antigenic and Immunogenic properties of Recombinant proteins consisting of two immunodominant African swine fever virus proteins fused with bacterial lipoprotein OprI. *Virol. J.* **19**, 16 (2022).
23. Gomez-Puertas, P. et al. Neutralizing antibodies to different proteins of African swine fever virus inhibit both virus attachment and internalization. *J. Virol.* **70**, 5689–5694 (1996).
24. Gómez-Puertas, P. et al. The African swine fever virus proteins p54 and p30 are involved in two distinct steps of virus attachment and both contribute to the Antibody-Mediated protective immune response. *Virology* **243**, 461–471. https://doi.org/10.1006/viro.1998.9068 (1998).
25. Escribano, J. M., Galindo, I. & Alonso, C. Antibody-mediated neutralization of African swine fever virus: Myths and facts. *Virus Res.* **173**, 101–109 (2013).
26. Sanchez, E. G., Perez-Nunez, D. & Revilla, Y. Development of vaccines against African swine fever virus. *Virus Res.* **265**, 150–155. https://doi.org/10.1016/j.virusres.2019.03.022 (2019).
27. Argilaguet, J. et al. Enhancing DNA immunization by targeting ASFV antigens to SLA-II bearing cells. *Vaccine* **29**, 5379–5385 (2011).
28. Murgia, M. V. et al. Evaluation of an African swine fever (ASF) vaccine strategy incorporating priming with an alphavirus-expressed antigen followed by boosting with attenuated ASF virus. *Arch. Virol.* **164**, 359–370 (2019).
29. Fang, N. et al. Expression and immunogenicity of Recombinant African swine fever virus proteins using the Semliki forest virus. *Front. Veterinary Sci.* **9**, 870009 (2022).
30. Goatley, L. C. et al. A pool of eight virally vectored African swine fever antigens protect pigs against fatal disease. *Vaccines* **8**, 234 (2020).
31. Buan, A. K. G., Reyes, N. A. L., Pineda, R. N. B. & Medina, P. M. B. In Silico design and evaluation of a multi-epitope and multi-antigenic African swine fever vaccine. *ImmunoInformatics* 8. https://doi.org/10.1016/j.immuno.2022.100019 (2022).
32. Zhang, L. Multi-epitope vaccines: a promising strategy against tumors and viral infections. *Cell. Mol. Immunol.* **15**, 182–184. https://doi.org/10.1038/cmi.2017.92 (2018).
33. Nguyen, T. L. et al. Designing a multi-epitope candidate vaccine by employing immunoinformatics approaches to control African swine fever spread. *J. Biomol. Struct. Dyn.* **41**, 10214–10229. https://doi.org/10.1080/07391102.2022.2153922 (2023).
34. Jia, N., Ou, Y., Pejsak, Z., Zhang, Y. & Zhang, J. Roles of African swine fever virus structural proteins in viral infection. *J. Vet. Res.* **61**, 135–143. https://doi.org/10.1515/jvetres-2017-0017 (2017).
35. Chong, L. C. & Khan, A. M. Vaccine target discovery. *Encyclopedia Bioinf. Comput. Biol.* 241 (2019).

36. Yu, M., Morrissy, C. J. & Westbury, H. A. Strong sequence conservation of African swine fever virus p72 protein provides the molecular basis for its antigenic stability. *Arch. Virol.* **141**, 1795–1802. https://doi.org/10.1007/bf01718302 (1996).
37. Dolata, K. M. et al. CP204L is a multifunctional protein of African swine fever virus that interacts with the VPS39 subunit of the homotypic fusion and vacuole protein sorting complex and promotes lysosome clustering. *J. Virol.* **97**, e01943–e01922 (2023).
38. de Villiers, E. P. et al. Phylogenomic analysis of 11 complete African swine fever virus genome sequences. *Virology* **400**, 128–136. https://doi.org/10.1016/j.virol.2010.01.019 (2010). https://doi.org/https://doi.org/
39. Singh, K., Barman, N. N., Buragohain, L., Kumar, S. & Malik, Y. S. Exploring In-Silico Immunoepitope landscape and genetic diversity in p72 and CD2v proteins across Asian African swine fever virus isolates. *Indian J. Microbiol.*, 1–13 (2024).
40. Argilaguet, J. M. et al. DNA vaccination partially protects against African swine fever virus lethal challenge in the absence of antibodies. (2012).
41. Ren, D. et al. Development and characterization of Recombinant ASFV CD2v protein nanoparticle-induced monoclonal antibody. *Int. J. Biol. Macromol.* **209**, 533–541. https://doi.org/10.1016/j.ijbiomac.2022.03.069 (2022).
42. Rodriguez, J. M., Garcia-Escudero, R., Salas, M. L. & Andres, G. African swine fever virus structural protein p54 is essential for the recruitment of envelope precursors to assembly sites. *J. Virol.* **78**, 4299–1313. https://doi.org/10.1128/jvi.78.8.4299-4313.2004 (2004).
43. Petrovan, V. *Antigenic Characterization of African Swine Fever Virus (ASFV) p30 and p54 Proteins* (Kansas State University, 2019).
44. Li, Z. et al. African swine fever virus: A review. *Life (Basel)* 12. https://doi.org/10.3390/life12081255 (2022).
45. Reis, A. L. et al. From structure prediction to function: defining the domain on the African swine fever virus CD2v protein required for binding to erythrocytes. *Mbio* **16**, e01655–e01624 (2025).
46. Dixon, L. K. et al. African swine fever virus proteins involved in evading host defence systems. *Vet. Immunol. Immunopathol.* **100**, 117–134 (2004).
47. Nguyen, G. T. et al. A plant-based oligomeric CD2v extracellular domain antigen exhibits equivalent immunogenicity to the live attenuated vaccine ASFV-G-Δ I177L. *Med. Microbiol. Immunol.* **213**, 22 (2024).
48. Song, J. et al. A candidate nanoparticle vaccine comprised of multiple epitopes of the African swine fever virus elicits a robust immune response. *J. Nanobiotechnol.* **21**, 424. https://doi.org/10.1186/s12951-023-02210-9 (2023).
49. Meza, B., Ascencio, F., Sierra-Beltran, A. P., Torres, J. & Angulo, C. A novel design of a multi-antigenic, multistage and multi-epitope vaccine against Helicobacter pylori: an in Silico approach. *Infect. Genet. Evol.* **49**, 309–317. https://doi.org/10.1016/j.meegid.2017.02.007 (2017).
50. Oli, A. N. et al. Immunoinformatics and vaccine development: an overview. *Immunotargets Ther.* **9**, 13–30. https://doi.org/10.2147/ITT.S241064 (2020).
51. Simbulan, A. M., Banico, E. C., Sira, E., Odchimar, N. M. O. & Orosco, F. L. Immunoinformatics-guided approach for designing a pan-proteome multi-epitope subunit vaccine against African swine fever virus. *Sci. Rep.* **14**, 1354. https://doi.org/10.1038/s41598-023-51005-3 (2024).
52. Salman, M. et al. The comparative Full-Length genome characterization of African swine fever virus detected in Thailand. *Animals* **14**, 2602 (2024).
53. Doytchinova, I. A. & Flower, D. R. VaxiJen: a server for prediction of protective antigens, tumour antigens and subunit vaccines. *BMC Bioinform.* **8**, 4. https://doi.org/10.1186/1471-2105-8-4 (2007).
54. Tahir et al. Epitope-based peptide vaccine design and target site depiction against middle East respiratory syndrome coronavirus: an immune-informatics study. *J. Translational Med.* **17**, 1–14 (2019).
55. Bui, H. H., Sidney, J., Li, W., Fusseder, N. & Sette, A. Development of an epitope conservancy analysis tool to facilitate the design of epitope-based diagnostics and vaccines. *BMC Bioinform.* **8**, 361. https://doi.org/10.1186/1471-2105-8-361 (2007).
56. Khan, M. et al. Immunoinformatics approaches to explore helicobacter pylori proteome (virulence factors) to design B and T cell multi-epitope subunit vaccine. *Sci. Rep.* **9**, 13321. https://doi.org/10.1038/s41598-019-49354-z (2019).
57. Khamjan, N. A., Lohani, M., Khan, M. F., Khan, S. & Algaissi, A. Immunoinformatics strategy to develop a novel universal multiple epitope-based COVID-19 vaccine. *Vaccines (Basel)* 11. https://doi.org/10.3390/vaccines11061090 (2023).
58. Weeratna, R. D., McCluskie, M. J., Xu, Y. & Davis, H. L. CpG DNA induces stronger immune responses with less toxicity than other adjuvants. *Vaccine* **18**, 1755–1762 (2000).
59. Martinez-Alonso, S., Martinez-Lopez, A., Estepa, A., Cuesta, A. & Tafalla, C. The introduction of multi-copy CpG motifs into an antiviral DNA vaccine strongly up-regulates its immunogenicity in fish. *Vaccine* **29**, 1289–1296. https://doi.org/10.1016/j.vaccine.2010.11.073 (2011).
60. Sun, X. et al. A CpG-riched plasmid as vaccine adjuvant reduce antigen dose of an inactivated Vibrio anguillarum vaccine in turbot (Scophthalmus Maximus L). *Fish. Shellfish Immunol.* **98**, 312–317. https://doi.org/10.1016/j.fsi.2020.01.031 (2020).
61. Ayyagari, V. S., Srirama, K. & T, C. V., K, A. P. & Design of a multi-epitope-based vaccine targeting M-protein of SARS-CoV2: an immunoinformatics approach. *J. Biomol. Struct. Dyn.* **40**, 2963–2977. https://doi.org/10.1080/07391102.2020.1850357 (2022).
62. Ebrahimi, M., Seyyedtabaei, S. J., Ranjbar, M. M. & Tahvildar-Biderouni, F. Javadi Mamaghani, A. Designing and modeling of multi-epitope proteins for diagnosis of Toxocara canis infection. *Int. J. Pept. Res. Ther.* **26**, 1371–1380 (2020).
63. Habib, A., Liang, Y., Xu, X., Zhu, N. & Xie, J. Immunoinformatic identification of multiple epitopes of gp120 protein of HIV-1 to enhance the immune response against HIV-1 infection. *Int. J. Mol. Sci.* **25** https://doi.org/10.3390/ijms25042432 (2024).
64. Shaw, D. E. et al. Atomic-level characterization of the structural dynamics of proteins. *Science* **330**, 341–346 (2010).
65. Ivanova, L. et al. Molecular dynamics simulations of the interactions between glial cell line-derived neurotrophic factor family receptor GFRα1 and small-molecule ligands. *ACS Omega*. **3**, 11407–11414 (2018).
66. Arumugam, S. & Varamballi, P. In-silico design of envelope based multi-epitope vaccine candidate against Kyasanur forest disease virus. *Sci. Rep.* **11**, 17118 (2021).
67. Wahl, S. M. & Rosenstreich, D. L. Role of B lymphocytes in cell-mediated immunity. I. Requirement for T cells or T-cell products for antigen-induced B-cell activation. *J. Exp. Med.* **144**, 1175–1187. https://doi.org/10.1084/jem.144.5.1175 (1976).
68. Wang, S. Y. & Weiner, G. Complement and cellular cytotoxicity in antibody therapy of cancer. *Expert Opin. Biol. Ther.* **8**, 759–768 (2008).
69. Schafer, A. et al. Adaptive cellular immunity against African swine fever virus infections. *Pathogens* **11** https://doi.org/10.3390/pathogens11020274 (2022).
70. Fagbohun, O. A. et al. Contriving a multi-epitope vaccine against African swine fever utilizing immunoinformatics. *Biomedical Res. Therapy*. **11**, 6642–6660 (2024).
71. Chen, T. Y. et al. Multi-epitope vaccine design of African swine fever virus considering T cell and B cell immunogenicity. *AMB Express*. **14**, 95 (2024).
72. Fleri, W. et al. The immune epitope database and analysis resource in epitope discovery and synthetic vaccine design. *Front. Immunol.* **8**, 278. https://doi.org/10.3389/fimmu.2017.00278 (2017).
73. Moldoveanu, S. C. & David, V. *Selection of the HPLC Method in Chemical Analysis* (eds Serban C. Moldoveanu & Victor David) 189–230 (Elsevier, 2017).
74. Idicula-Thomas, S. & Balaji, P. V. Understanding the relationship between the primary structure of proteins and its propensity to be soluble on overexpression in Escherichia coli. *Protein Sci.* **14**, 582–592 (2005).
75. Guruprasad, K., Reddy, B. B. & Pandit, M. W. Correlation between stability of a protein and its dipeptide composition: a novel approach for predicting in vivo stability of a protein from its primary sequence. *Protein Eng. Des. Selection*. **4**, 155–161 (1990).

76. Ubi, G. M., Ikpeme, E. V. & Essien, I. S. *Data Science for COVID-19* (eds Utku Kose, Deepak Gupta, Victor Hugo C. De Albuquerque, & Ashish Khanna) 1–25 (Academic, 2022).
77. Chang, K. Y. & Yang, J. R. Analysis and prediction of highly effective antiviral peptides based on random forests. *PloS One*. **8**, e70166 (2013).
78. Enayatkhani, M. et al. Reverse vaccinology approach to design a novel multi-epitope vaccine candidate against COVID-19: an in Silico study. *J. Biomol. Struct. Dynamics*. **39**, 2857–2872 (2021).
79. Rath, A., Davidson, A. R. & Deber, C. M. The structure of unstructured regions in peptides and proteins: role of the polyproline II helix in protein folding and recognition. *Pept. Science: Original Res. Biomolecules*. **80**, 179–185 (2005).
80. Qiao, X., Qu, L., Guo, Y. & Hoshino, T. Secondary structure and conformational stability of the antigen residues making contact with antibodies. *J. Phys. Chem. B*. **125**, 11374–11385 (2021).
81. Branden, C. I. & Tooze, J. *Introduction To Protein Structure* (Garland Science, 2012).
82. Omar, S. et al. *IOP Conference Series: Materials Science and Engineering* 012025 (IOP Publishing).
83. Laskowski, R. A., Furnham, N. & Thornton, J. M. *Biomolecular Forms and Functions: a Celebration of 50 Years of the Ramachandran Map* 62–75 (World Scientific, 2013).
84. DasGupta, D., Kaushik, R. & Jayaram, B. From Ramachandran maps to tertiary structures of proteins. *J. Phys. Chem. B*. **119**, 11136–11145 (2015).
85. Torshin, I. Y., Esipova, N. G. & Tumanyan, V. G. Alternatingly twisted β-hairpins and nonglycine residues in the disallowed II′ region of the Ramachandran plot. *J. Biomol. Struct. Dynamics*. **32**, 198–208 (2014).
86. Desta, I. T., Porter, K. A., Xia, B., Kozakov, D. & Vajda, S. Performance and its limits in rigid body Protein-Protein Docking. *Structure* **28**, 1071–1081e1073. https://doi.org/10.1016/j.str.2020.06.006 (2020).
87. Sanami, S. et al. Design of a multi-epitope vaccine against cervical cancer using immunoinformatics approaches. *Sci. Rep.* **11**, 12397 (2021).
88. Miao, C. et al. Identification of p72 epitopes of African swine fever virus and preliminary application. *Front. Microbiol.* **14**, 1126794 (2023).
89. Zheng, N. et al. A novel linear B-cell epitope on the P54 protein of African swine fever virus identified using monoclonal antibodies. *Viruses* **15** https://doi.org/10.3390/v15040867 (2023).
90. Goatley Lynnette, C. & Dixon Linda, K. Processing and localization of the African swine fever virus CD2v transmembrane protein. *J. Virol.* **85**, 3294–3305. https://doi.org/10.1128/jvi.01994-10 (2011).
91. Hu, C. et al. In vitro SELEX and application of an African swine fever virus (ASFV) p30 protein specific aptamer. *Sci. Rep.* **14**, 4078. https://doi.org/10.1038/s41598-024-53619-7 (2024).
92. Raoufi, E. et al. Epitope prediction by novel immunoinformatics approach: a state-of-the-art review. *Int. J. Pept. Res. Ther.* **26**, 1155–1163 (2020).
93. Savransky, V. et al. Correlation between anthrax lethal toxin neutralizing antibody levels and survival in guinea pigs and nonhuman primates vaccinated with the AV7909 anthrax vaccine candidate. *Vaccine* **35**, 4952–4959. https://doi.org/10.1016/j.vaccine.2017.07.076 (2017).
94. Ouyang, K. et al. Comparative analysis of routes of immunization of a live Porcine reproductive and respiratory syndrome virus (PRRSV) vaccine in a heterologous virus challenge study. *Vet. Res.* **47**, 45. https://doi.org/10.1186/s13567-016-0331-3 (2016).
95. Tudor, D. et al. TLR9 pathway is involved in adjuvant effects of plasmid DNA-based vaccines. *Vaccine* **23**, 1258–1264. https://doi.org/10.1016/j.vaccine.2004.09.001 (2005). https://doi.org/https://doi.org/
96. Murray, S. M. et al. The impact of pre-existing cross-reactive immunity on SARS-CoV-2 infection and vaccine responses. *Nat. Rev. Immunol.* **23**, 304–316. https://doi.org/10.1038/s41577-022-00809-x (2023).
97. Baseer, S., Ahmad, S., Ranaghan, K. E. & Azam, S. S. Towards a peptide-based vaccine against Shigella sonnei: A subtractive reverse vaccinology based approach. *Biologicals* **50**, 87–99 (2017).
98. Kang, T. H. & Seong, B. L. Solubility, stability, and avidity of Recombinant antibody fragments expressed in microorganisms. *Front. Microbiol.* **11**, 1927 (2020).
99. Alberts, B. et al. *Molecular Biology of the Cell*. 4th Edition (Garland Science, 2002).
100. Akkaya, M., Kwak, K. & Pierce, S. K. B cell memory: Building two walls of protection against pathogens. *Nat. Rev. Immunol.* **20**, 229–238 (2020).
101. Ros-Lucas, A., Correa-Fiz, F., Bosch-Camós, L., Rodriguez, F. & Alonso-Padilla, J. Computational analysis of African swine fever virus protein space for the design of an epitope-based vaccine ensemble. *Pathogens* **9**, 1078 (2020).
102. Munoz, A. L. & Tabares, E. Characteristics of the major structural proteins of African swine fever virus: role as antigens in the induction of neutralizing antibodies. A review. *Virology* **571**, 46–51. https://doi.org/10.1016/j.virol.2022.04.001 (2022).
103. Zhou, P. et al. Deletion of the H240R gene of African swine fever virus decreases infectious progeny virus production due to aberrant virion morphogenesis and enhances inflammatory cytokine expression in Porcine macrophages. *J. Virol.* **96**, e01667–e01621 (2022).
104. Zheng, X., Nie, S. & Feng, W. H. Regulation of antiviral immune response by African swine fever virus (ASFV). *Virol. Sin.* **37**, 157–167 (2022).
105. Fan, R. et al. Development of novel monoclonal antibodies for blocking NF-κB activation induced by CD2v protein in African swine fever virus. *Front. Immunol.* **15**, 1352404 (2024).
106. Wu, P. et al. Antigenic regions of African swine fever virus phosphoprotein P30. *Transbound. Emerg. Dis.* **67**, 1942–1953 (2020).
107. Jia, N., Ou, Y., Pejsak, Z., Zhang, Y. & Zhang, J. Roles of African swine fever virus structural proteins in viral infection. *J. Veterinary Res.* **61**, 135–143 (2017).
108. Weng, C. Current research progress on the viral immune evasion mechanisms of African swine fever. *Anim. Dis.* **4**, 18 (2024).

Author contributions

D.V. was involved in conceptualization, methodology, analysis and validation, writing the first draft. D.N. supervised the whole research and was involved in conceptualization and funding acquisition. Q.A.N. and W.A. performed the formal analysis. A.P. and R.S. contributed for the methodology and revision of manuscript. A.T. supervised the research. All authors reviewed the manuscript.

Funding

The author(s) acknowledge receiving financial support for this academic work's research and publication. D.V. received scholarship from The Second Century Fund (C2F), Chulalongkorn University. D.N. received the financial support from Thailand Science Research and Innovation Fund at Chulalongkorn University, Agricultural Research Development Agency (ARDA) and Chulalongkorn University for the Research Unit: Swine Viral Evolution and Vaccine Development Research Unit (GRU 6502731003-1).

Declarations

Competing interests
The authors declare no competing interests.

Additional information
Correspondence and requests for materials should be addressed to D.N.

Reprints and permissions information is available at www.nature.com/reprints.

Publisher's note Springer Nature remains neutral with regard to jurisdictional claims in published maps and institutional affiliations.